

THE POTENTIAL FOR GENISTEIN, A TOPISOMERASE II INHIBITOR,
TO INDUCE INTER-CHROMOSOMAL HOMOLOGOUS RECOMBINATION

by

Caroline French

A thesis submitted to the faculty of
The University of North Carolina at Charlotte
in partial fulfillment of the requirements
for the degree of Master of Science in
Biology

Charlotte

2023

Approved by:

DR. CHRISTINE RICHARDSON

Dr. Junya Tomida

Dr. Yvette Huet

ABSTRACT

CAROLINE FRENCH. The Potential for Genistein, a Topoisomerase II Inhibitor, to Induce Inter-Chromosomal Homologous Recombination. (Under the Direction of DR. CHRISTINE RICHARDSON.)

Maintenance of genome integrity is important for preventing mutagenic events and preserving overall cell functionality. DNA damaging agents induce DNA double strand breaks (DSBs) that are repaired through repair pathways non-homologous end-joining (NHEJ) and homologous recombination (HR). DSB-induced inter-chromosomal HR repair can lead to mutagenic events including the translocations associated with infant acute myeloblastic leukemia (AML) and infant acute lymphoblastic leukemia (ALL). It has been cited that a specific translocation associated with AML involving the human *MLL* gene at the 11q23 chromosome position is associated with exposure to topoisomerase II (Top2) poison etoposide.. The natural compounds known as bioflavonoids have cardioprotective, cytoprotective, anti-inflammatory, anti-viral, and anticarcinogenic properties at low doses and are added to many over the counter supplements. However, they are also biochemically similar to etoposide and inhibit Top2 and cause DNA DSBs in a dose-dependent manner in cultured cells. Previous work supports the potential for *in vivo* exposure to bioflavonoid genistein to cause DNA damage in mice and rats, and is associated with a dose-dependent increase of cells in S phase hypothesized to be associated with frozen Top2 cleavage complexes halting the cell cycle. Further, bioflavonoids are capable of crossing the placental barrier and may pose a threat to a developing fetal genome. This work utilized a unique transgenic reporter mouse model to be the first study to evaluate genistein for its direct potential to promote DSB-induced inter-chromosomal homologous recombination *in vivo*. It was observed that genistein induces inter-chromosomal HR at readily detectable frequency in the kidney, uterus, testes, and placenta but minimally or undetectable in the bone marrow, liver, or *in utero* in developing whole fetus or fetal liver. This work is the first demonstration that genistein supplementation *in vivo* can cause inter-chromosomal HR. This implies a more mutagenic role of

genistein has previously been described and serves as important evidence that genistein supplementation should be moderated.

ACKNOWLEDGEMENTS

In my graduate career I have had the unending support of my principal investigator Dr. Christine Richardson. Her mentorship, guidance, and expertise have been indispensable during my work. I have always appreciated that she took a chance on an undergraduate student coming from a small biology program, and gave me the opportunity to experience graduate research. In all the days of lab work, I thank her for developing my critical thinking skills, problem solving abilities, and passion for molecular biology. I hope I am engaging in work that makes her proud after my time in her lab.

I thank my committee members Dr. Junya Tomida and Dr. Yvette Huet for their incredible suggestions and feedback throughout the development of my project. Their perspectives have opened up many doors in this work, and presented insightful contributions. Further, their kindness and empathy as supportive committee members must be recognized for it goes above and beyond. I will always remember their consideration.

I would also like to acknowledge my incredible post-doc, Dr. Donna Goodenow for her support, advice, and mentorship. Her help at the next bench over has molded me for the better. I would also like to thank Kiran Lalwani who is worth her weight in gold for her knowledge, patience, and curiosity. She welcomed me with open arms to the lab, and is every representation of a fantastic scientist, teacher, and friend. Further I would like to recognize Lori Unger for her partnership and work in the lab as she grows into an independent researcher. I also thank our undergraduates Jordan Foster, Jen Heald, Elizabeth Toufekoulas, Joeley Seitz, Henry Thompson, and Heather Derby for getting excited about this work with me, and helping around the lab. In the department I acknowledge the incredible faculty that make this department as strong as it is, with special thanks to Dr. Adam Reitzel for his support of the graduate students, Dr. Michelle Pass for her mentorship in teaching, and Dr. Kristen Funk, and her lab, for sharing their knowledge and expertise.

Outside of UNC Charlotte I acknowledge my undergraduate research mentor, Dr. George Argyros for always pushing me to learn more, and better myself as a scientist.

DEDICATION

I dedicate my Master's thesis work to my parents, Robert and Mary French, and my little brother, Sean French. I cherish them more than I could put into words. I also dedicate my work to my dog, Rocket, who was the most loyal companion a graduate student could have.

TABLE OF CONTENTS

LIST OF FIGURES	x
FREQUENTLY USED ABBREVIATIONS	xi
CHAPTER 1: INTRODUCTION	
1.1 An introduction to DNA Damage and Repair	1
1.2 Double Strand Break (DSB) Repair	2
1.2.1 Non-Homologous End-Joining	3
1.2.2 Homologous Recombination	5
1.3 Meiotic Recombination	8
1.4 Topoisomerases and Disruptions in DSB Repair	9
1.5 Natural Compounds, Bioflavonoids, and their ability to disrupt Top2	13
1.6 Literature Review of Genistein Research	15
1.7 Hypothesis and Aims	16
CHAPTER 2: MATERIALS AND METHODS	
2.1 The Transgenic Rainbow Mouse Model to Study Inter-chromosomal HR	18
2.2 Embryonic Stem Cell Culture and Genistein Treatment	19
2.3 PCR and Genotyping	19
2.4 Primary MEFs Culture and Treatment	20
2.5 Genistein Treatment Protocol	21
2.6 Mouse Perfusion	21
2.7 Organ Isolation and Fixation for FACS	22
2.8 Organ Isolation and Fixation for ImageStream X Analysis	23
2.9 Hoechst Staining	23
2.10 Embedding and Cryosectioning	24
2.11 Hematoxylin and Eosin Staining	25
2.12 Immunohistochemistry	26

CHAPTER 3: RESULTS	28
3.1 Validation of Rainbow Mouse Model and DSB-induced Inter-chromosomal HR	28
3.2 Induction of Inter-chromosomal HR in Proliferative and Filtering Organs by Genistein	29
3.3 Induction of Inter-chromosomal HR in utero by Genistein	33
3.4 Induction of Inter-chromosomal HR in Reproductive Organs and Meiotic Tissue by Genistein	35
CHAPTER 4: DISCUSSION	39
4.1 Filtering and Proliferative Organs	39
4.2 In-utero	41
4.3 Spermatocytes	42
4.4 Uterus	44
4.5 Significance and Implications	45
REFERENCES	47

LIST OF FIGURES

FIGURE 1: Double-Strand Break Repair: Non-homologous End-Joining	3
FIGURE 2: Double-Strand Break Repair: Homologous Recombination	5
FIGURE 3: Topoisomerase II and Replication	11
FIGURE 4: The Rainbow Mouse Model	19
FIGURE 5: PCR of the Rainbow Mouse Model Constructs	29
FIGURE 6: Mouse Embryonic Fibroblasts Treated with Genistein	29
FIGURE 7: Genistein Treatment <i>in vivo</i> : Immunohistochemistry of the Adult Mouse Kidney	30
FIGURE 8: Genistein Treatment <i>in vivo</i> : Flowcytometry of the Adult Mouse Kidney	31
FIGURE 9: Genistein Treatment <i>in vivo</i> : Immunohistochemistry of the Adult Mouse Liver	32
FIGURE 10: Genistein Treatment <i>in vivo</i> : Flowcytometry of the Adult Mouse Liver	33
FIGURE 11: Genistein Treatment <i>in vivo</i> : Flowcytometry of the Adult Mouse Bone Marrow	34
FIGURE 12: Genistein Treatment <i>in utero</i> : Flowcytometry of Whole Fetal Tissue	34
FIGURE 13: Genistein Treatment <i>in utero</i> : Flowcytometry of the Fetal Liver	35
FIGURE 14: Genistein Treatment <i>in utero</i> : Flowcytometry of the Placenta	35
FIGURE 15: Genistein Treatment <i>in vivo</i> : Flowcytometry of the Adult Mouse Testes	36
FIGURE 16: Genistein Treatment <i>in vivo</i> : Immunohistochemistry of the Adult Mouse Testes	37
FIGURE 17: Genistein Treatment <i>in vivo</i> : RAD51 Expression in the Adult Mouse Testes	38
FIGURE 18: Genistein Treatment <i>in vivo</i> : Immunohistochemistry of the Adult Mouse Uterus	39

FREQUENTLY USED ABBREVIATIONS

DNA: Deoxyribonucleic Acid

DSB: Double strand break

HR: Homologous Recombination

NHEJ: Non-homologous end-joining

MEFs: Mouse Embryonic Fibroblasts

GFP: Green Fluorescent Protein

IHC: Immunohistochemistry

FACS: Fluorescence-activated cell sorting

CHAPTER 1: INTRODUCTION

1.1 An Introduction to DNA Damage and Repair

Deoxyribonucleic acid (DNA) is the genetic material responsible for development, function, and reproduction of all living organisms. Maintenance of genome integrity is important for preventing mutagenic events and preserving overall cell functionality. DNA is constantly exposed to endogenous and exogenous agents that can compromise its integrity. Damaged DNA unrepaired or incorrectly repaired can lead to the development of mutations, genomic instability, and potentially contribute to the onset of certain diseases such as neurodegenerative conditions and cancer¹⁻³. There are many types of DNA damage, which include DNA single-strand breaks (SSBs), DNA double-strand breaks (DSBs), DNA base modifications, DNA adducts, and DNA crosslinks. SSBs describe the breakage of one of the two strands of DNA, whereas DSBs break both strands. Base modifications engage with the DNA via a chemical modification of the nucleotide bases, through processes including oxidation and/or methylation. The addition of chemical groups via a covalent bond is a DNA adduct, while covalent bonds between two DNA strands, or DNA with other molecules, are called crosslinks. Mechanisms of endogenous DNA damage include spontaneous hydrolysis, reactive oxygen species byproducts of cellular metabolism, and DNA replication errors. Exogenous sources of DNA damage include exposure to ionizing radiation via X-rays and gamma rays, ultraviolet (UV) radiation, environmental chemical compounds, as well as drugs and toxins. Cells have multiple DNA damage detection and repair pathway mechanisms to tolerate this damage, as well as maintain genome stability. Together, the processes enacting this detection, signaling, and repair are called the DNA damage response (DDR)^{1; 3-5}. These systems work together to preserve the cell's functionality or initiate apoptosis in the case of irreparable or overwhelming numbers of lesions.

The initiation of the DNA damage response requires detector proteins to identify the lesions. Major proteins in the initiation of the DDR include the ataxia-telangiectasia mutated (ATM) and ATM-Rad3-Related (ATR) kinases whose activation triggers a phosphorylation signaling cascade that activates checkpoint kinases, specifically CHk1 and CHk2, that stall cell cycle progression while repair occurs¹. Repair pathway choice is determined by the type of break, as well as other more debated factors in the field of DNA damage repair including cell cycle stage, location, and frequency. SSB repair pathways include base excision repair (BER), nucleotide excision repair (NER), and mismatch repair (MMR). DSB repair pathways include homologous recombination (HR), and non-homologous end-joining (NHEJ)^{1; 4}.

If DNA damage is severe or cannot be repaired, cells may undergo programmed cell death, known as apoptosis, to prevent the retention and replication of damaged genetic material. Although there are many modes of DNA repair, errors can still occur, leading to mutations and genomic instability. Additionally, if the DNA damage exceeds the cell's tolerance for damage and ability to repair, the damage can have detrimental effects on cellular function and potentially contribute to the development of diseases, including cancer. Overall, genomic instability has significant consequences for the cell and organism^{1; 4; 12; 13}.

1.2 Double Strand Break (DSB) Repair

There are two prominent pathways for DSB repair: NHEJ and HR. These pathways work to maintain genomic integrity, and pathway choice is determined by many different factors including cell cycle stage, cell type, and location or frequency of the damage. Some questions about repair pathway choice remain debated in the field, and work is ongoing to elucidate other factors that aid in determining repair pathway choice in the cell^{1; 14}.

1.2.1 Non-Homologous End-Joining

NHEJ is an error-prone, fast repair DSB repair pathway but does not require a region of sequence homology. Ku70/80, recognition proteins, identify and bind to the DNA ends, recruiting the essential NHEJ factors including DNA-PKcs. The ends are processed by MRN, CtIP, and Artemis, and ligated by the DNA ligase IV complex (Ligase 4, XRCC4, and XLF; LigIV)^{9; 11}. NHEJ is a prevalent mechanism in both prokaryotes and eukaryotes, and involves several distinct steps, including DNA end recognition, DNA end processing, alignment of broken ends, and ligation¹⁵.

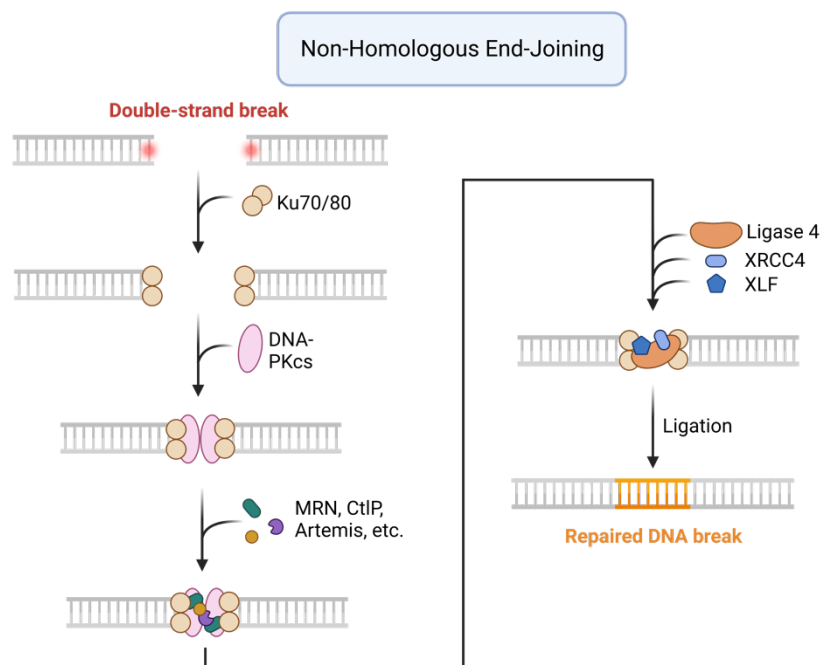


Figure 1. A diagram illustrating the non-homologous end-joining (NHEJ) pathway of DNA repair. The initial step in this pathway involves recognition of the double-stranded break in DNA by the NHEJ complex. Once recognized, these damaged DNA ends are trimmed by end processing. Processed DNA ends are brought into close proximity for proper alignment which allows for ligation without the need for a homologous template. This process helps maintain genomic stability by repairing double-stranded breaks, but may result in insertions or deletions in the repaired DNA.

The first step in NHEJ is the recognition of DNA ends by the Ku protein heterodimer (Ku70/Ku80). The Ku protein binds to the DNA ends, forming a stable complex and protecting them from degradation. Upon recognition and binding the Ku-DNA complex serves as a scaffold for the

recruitment of other NHEJ factors to the site of DNA damage. The Ku protein also functions as an anchor for the DNA-dependent protein kinase catalytic subunit, DNA-PKcs, which is attracted to the Ku-DNA ends. When the DNA-PKcs binds with the Ku-DNA complex forming the DNA-PK complex. Many DSBs present with ends that are not compatible with each other, and would result in significant mutations or unequal lengths for pairing, and nucleases work to resolve this strand disagreement. After the DNA ends are recognized by the Ku protein, they undergo break end processing in a blunting step, often via the Artemis nuclease, to prepare them for ligation. This processing step involves the removal of damaged or incompatible DNA ends, as well as the modification of the DNA ends to promote their alignment. Once the DNA ends are processed, the broken ends need to be aligned to allow for proper ligation. DNA-PKcs and XRCC4-like factor (XLF) engage in the ligation mechanism and facilitate the end-to-end joining of the processed DNA ends. XLF acts as a bridge between the DNA ends, promoting alignment and stabilization of the protein-DNA complex. Following alignment, the final step of NHEJ is the ligation of the DNA ends. LigIV catalyzes the formation of a phosphodiester bond between the DNA ends, sealing the break and restoring the integrity of the DNA molecule. XRCC4 acts as a scaffold protein, facilitating the recruitment and activation of LigIV¹⁵.

Although NHEJ is a highly efficient repair pathway and can function in all phases of the cell cycle, it can lead to errors, such as small insertions or deletions at the site of repair. These alterations, known as insertions or deletions (indels), can result from the misalignment alignment of DNA ends during repair. Indels can have varying effects on the function of the repaired gene, ranging from no impact to complete loss of function. NHEJ is not only involved in the repair of DNA breaks, but it also participates in other important cellular processes. For example, during V(D)J recombination, NHEJ plays a critical role in the generation of diverse antibody and T-cell receptor genes. V(D)J recombination involves the rearrangement of gene segments to produce a vast repertoire of antigen

receptor genes. NHEJ brings together different gene segments, allowing their precise joining and the subsequent generation of a functional gene¹⁵.

1.2.2 Homologous Recombination

HR is a vital process that occurs in cells to repair damaged DNA, ensure genetic diversity, and facilitate the exchange of genetic information between homologous chromosomes. It is a complex molecular mechanism that involves the precise exchange of genetic material between two DNA molecules or sister chromatids. In this process, similar or identical sequences of DNA are aligned and exchanged, resulting in the formation of hybrid DNA molecules. HR plays a crucial role in various biological processes, including DNA repair, meiosis, and the generation of genetic diversity¹⁶. HR is most active during stages of the cell cycle (S/G2/M) where sister chromatids are present, and most active during the S phase. During G1, where no sister chromatids are present, there is an active inhibition of HR⁸⁴.

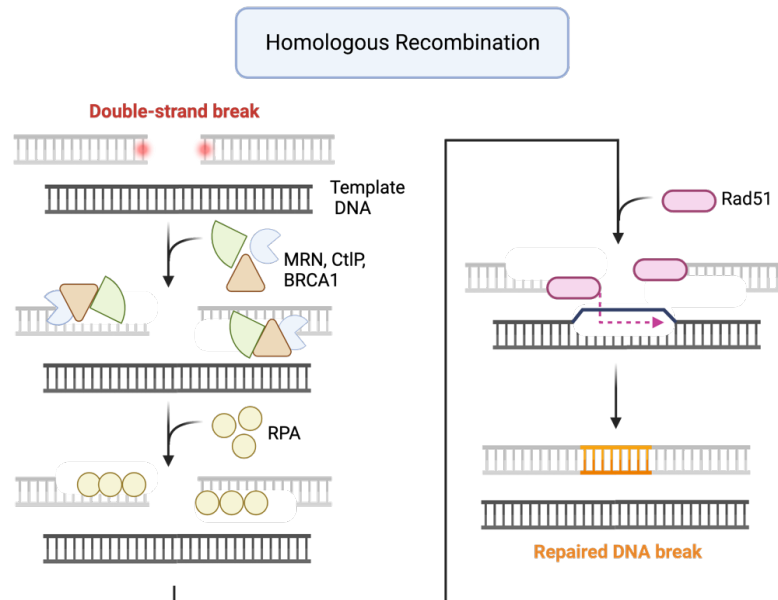


Figure 2. A diagram illustrating the homologous recombination process of DNA repair. When a double strand break occurs in DNA, the broken ends are resected in a 5' to 3' direction generating single-strand overhangs. These overhangs find homologous sequences in the sister chromatid and invade intact DNA to form displacement loops. The damaged DNA is repaired using the homologous sequence as a template. During this step, exchange of genetic material occurs between the two DNA strands, and the template sequence is copied.

The three major steps of HR include pre-synapsis, synapsis, and post-synapsis (figure 2). Pre-synapsis includes 5'-3' end resection that creates a 3' single-stranded DNA overhang. This overhang invades the template strand during synapsis, creating a Holliday junction, and the template sequence is copied. Then, the DNA ends are ligated and the break is resolved^{9; 10}. The process of HR begins with the recognition and pairing of homologous DNA sequences. These sequences can be found on the sister chromatid, homologous chromosome, or within repetitive sequences located on different chromosomes. The initial step involves the formation of a DNA double-strand break (DSB) at one of the participating DNA molecules. This break can be induced by external factors such as radiation or chemical agents, or it can occur spontaneously during DNA replication or other cellular processes¹⁷. Once a DNA DSB occurs, it triggers a cascade of events that lead to the repair of the break by HR. The broken DNA molecule is initially processed by nucleases, which trim the broken ends in a 5'-3' end resection to generate ssDNA overhangs. This resection occurs during presynapsis in two major steps starting with the MRN complex and CtIP in human cells. The MRN complex is composed of three subunits Mre11, Rad50, and Nbs1 in humans^{18; 19}. Mre11 contains intrinsic DNA binding activity, and endo/exonuclease activities against DNA substrates, but not the 5'-3' activity seen in the early resection steps of HR²⁰. The recruitment of the MRN complex results in the activation of the MRE11 nuclease for resection toward the break end, creating a short 3' ssDNA overhang. This cleavage, occurring away from the break end, allows the resection complexes to avoid the end-binding proteins including topoisomerases or Ku. These ssDNA overhangs then search for complementary sequences on the intact DNA molecule, leading to the formation of a nucleoprotein filament. This filament is assembled by RecA in bacteria or Rad51 in eukaryotes. In HR RAD51 is the protein in mitotic cells HR responsible for creating a connection to the DNA and conducting homology search using the RAD51 right-handed helical filament on the ssDNA. The RAD51 filament nucleation occurs, and RAD51 filament growth is supported by mediators RAD52 and BRCA2 which assist in the promotion of RAD51 function. Replication

associated protein A (RPA) coats the DNA and preferentially binds ssDNA in eukaryotes. RPA is in competition with RAD51, and inhibits RAD51's presynaptic filament function. Mediator proteins Rad55 and Rad57 are responsible for ensuring RAD51 can overcome the inhibitory nature of RPA in *Saccharomyces cerevisiae*, and the proteins with overlapping functions to these mediators in mammals have not been completely elucidated. Other yeast mediator proteins include Rad52 which is capable of annealing homologous ssDNA that is coated by RPA. Human Rad52 has not been observed to have this same functionality¹⁷. In mammals BRCA2 operates with similar function²¹. BRCA2 is a necessary protein for RAD51 filament formation and binds RAD51 through the BRC repeat domain and the CTRB domain¹⁷. BRCA2 is cited as related to RAD51 filament formation, as well as nucleation and stabilization of the presynaptic filament. These functions deem BRCA2 as a RAD51 mediator that helps RAD51 overcome the inhibitory nature of RPA^{21;17}. . The three major steps of HR include pre-synapsis, synapsis, and post-synapsis. Pre-synapsis includes 5-3' end resection that creates a 3' single-stranded DNA overhang. This overhang invades the template strand during synapsis, creating a Holliday junction, and the template sequence is copied. Then, the DNA ends are ligated and the break is resolved^{9; 10}.

Postsynapsis there are several possible pathways including synthesis-dependent strand annealing (SDSA), break-induced replication (BIR), and Holliday Junction formation and resolution. Both SDSA and BIR result in non-crossover outcomes and both can result in loss of heterozygosity (LOH). The strand invading and creating the D loop intermediate in SDSA becomes disengaged after the DNA is synthesized, and annealed with the second end. This annealing results in a local conversion. BIR results in the development of a complete replication fork from the D-loop, and the chromosome undergoes replication using the template chromosome. Holliday Junction resolution can result in both a crossover event or a non-crossover event, and both ends of the break are actively involved with the repair process²². Crossover events can result in genome rearrangements including translocations, deletions, amplifications, and inversions^{16;23}. Two

DSBs in the genome on different chromosomes can result in inter-chromosomal recombination promoting the formation of translocations and can act as a source of cancer-inducing mutagenesis⁸⁴.

Early work identifying HR-related mutagenesis was performed in yeast, and showed that stress influences the reliability of HR. Bloom syndrome, Fanconi anemia, and several cancers including hereditary breast and ovarian cancers are related to mutations in genes important for the HR pathway^{16; 20;17}.

1.3 Meiotic Recombination

Meiosis is an important molecular process responsible for a significant amount of genetic variation and the production of fertile gametes in many species. Meiosis includes chromosome segregation in two steps; first, a separation of homologous chromosomes, and second, a separation of the sister chromatids. In the first round of division, bivalents, the pairing of homologous chromosomes, are created. Meiosis in many species requires a crossover event, which is an exchange of two non-sister chromatids from homologous chromosomes. This crossing over, for each bivalent, is an obligatory step facilitating the production of viable gametes. HR outcomes in meiosis include large, reciprocal crossovers between homologous chromosomes, and non-crossovers resulting in the smaller, segmental and non-reciprocal DNA replacement event where a homologous sequence has been inserted¹⁸. The initiation of meiotic recombination is rooted in genetically programmed DNA lesions. PRDM9 is a histone methyltransferase that binds DNA as an early recombination step. In a few hundred of these PRDM9-DNA binding interactions SPO11 catalyzes DNA cleavage creating a DSB in meiotic recombination¹⁸. The DNA ends undergo resection, 5' to 3', and 3' ssDNA overhands are produced. RPA binds the ssDNA, and is preferentially replaced by DMC1 and RAD51. DMC1 and RAD51, bound to the ssDNA, create nucleoprotein filaments. These nucleoprotein filaments act as a protein scaffold preparing DNA for a recombination event and strand exchange¹⁹.

Although RAD51 is expressed in both mitotic and meiotic cells, DMC1 is only expressed in meiosis. RAD51 and DMC1 bind ssDNA on the DSB-initiating chromosome only, whereas RPA binds the DSB-initiating and repair template chromosomes. The occupation of the ssDNA overhang has DMC1 preferentially occupying the end of the overhang closest to the break site. DMC1 and RAD51 replace RPA from nascent ssDNA overhangs. It is proposed that RPA, which remains bound on the template chromosome at this point, is stabilizing the D-loop formed during strand invasion, and creating a recombination intermediate¹. In meiosis, the non-sister homologous chromosome, rather than the sister chromatid, is used as a repair template. This preferential step favoring the homologous chromosome as a repair partner is required for crossover events to occur. Homology search enzymes from the Rad51 filament are thought to be responsible for facilitating the homologous template preference¹⁸.

1.4 Topoisomerases and Disruptions in DSB Repair.

DNA has the propensity to become tangled and can develop supercoils under the pressure of essential cellular processes like DNA replication, transcription, recombination, and chromosome segregation. Topoisomerases are a group of enzymes whose function is to change the topology of DNA to alleviate helical torsion, supercoils, and tangling during these processes^{24; 25}. Topoisomerases introduce transient DNA breaks to resolve knots and facilitate the separation of DNA strands. Two major classes of topoisomerases include type I and type II. Type I topoisomerases create transient single-strand breaks in the DNA molecule, while type II topoisomerases completely cleave both DNA strands. Both types of topoisomerases are essential for maintaining the integrity and proper functioning of the genome²⁴⁻²⁶.

Type I topoisomerases include DNA topoisomerase I which binds to DNA, cuts a singular strand, and creates a covalent bond with the 5' DNA end via a phosphodiester bond. Then, the DNA strand rotates as the enzyme passes the intact strand through the break. DNA topoisomerase I then reseals

the DNA strand, which completes the relaxation of either positive or negative supercoiling²⁷. More complex processes, like DNA replication, chromosome condensation, and decatenation, often require topoisomerase class II mechanisms for torsion relief. A DSB is created, and the neighboring strand is passed through the duplex in the gate mechanism that requires ATP hydrolysis to occur. The break is then ligated, and helical torsion has been resolved^{12; 27; 28}.

Topoisomerase II (Top2) is responsible for cleaving both DNA strands of DNA in an effort to maintain genome integrity, regulate DNA topology, and protect mechanisms like cell division. In mitotic cells Top2 is essential for DNA replication, chromosome condensation, and segregation; Top2 is critical for faithful and accurate cell division. DNA replication occurs in S phase, and the entire genome is replicated in preparation for cell division. As the replication fork proceeds, the DNA helix ahead of the replication fork experiences over-winding due to the mechanism of the DNA polymerases unwinding the DNA preceding it. Over-winding can lead to positive supercoils that can stall the replication process. Here, Top2 initiates its torsion-resolution mechanism by introducing transient DSBs (figure 3). After the tension is relieved, via the gate mechanism, strand passing, the DNA is ligated by Top2 and the replication machinery can continue to progress down the continuous DNA strands^{26; 29; 30}.

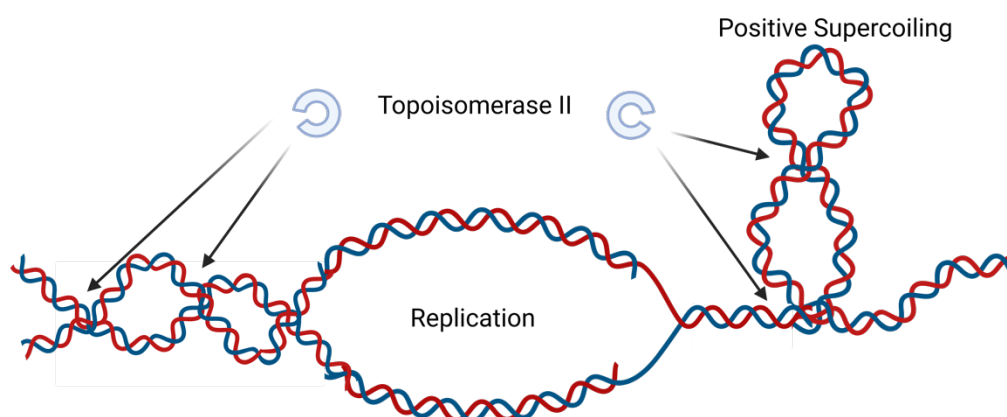


Figure 3. The role of topoisomerase II in relaxing supercoils in DNA replication.

During metaphase chromosomes must condense to facilitate proper chromosome alignment and segregation during anaphase and cell division. Top2's role in chromosome condensation is resolving catenated, intertwined sister chromosomes. Cohesin proteins hold the sister chromatids together during condensation, and Top2 introduces transient DSBs between them, allowing for the passage of one chromatid through the other in a mechanism called decatenation. The cell then enters metaphase, and the chromosomes align at the cell's equatorial plate. Top2 resolves entanglements or knots that occur during this process to ensure proper alignment, and prevention of mis-segregation and aneuploidy events leading to potential adverse effects on cell and organism development and/or health^{30; 31}.

During meiosis Top2 plays an essential role in the regulation of DNA topology via its contribution to accurate DNA recombination, chromosome segregation, and the maintenance of genome integrity. During the alignment of the homologous chromosomes, Top2 creates transient DSBs that allow for the genetic exchange to occur and ensures that the breaks are resolved. Top2 plays a role in segregation of the homologous chromosomes during disjunction in meiosis I by engaging in decatenation and resolution of DNA tangles similar to the mechanism of Top2 in mitosis^{18; 32-34}.

The importance of topoisomerases is evident in their essential roles in DNA metabolism and cell viability. Genetic defects or the inhibition of topoisomerase activity can have severe consequences. Inhibition of topoisomerases is a therapeutic strategy in cancer treatment²⁸. Certain chemotherapeutic drugs are topoisomerase inhibitors (e.g., etoposide, doxorubicin) and act by targeting topoisomerases and preventing them from resealing DNA breaks, leading to the accumulation of DNA damage and cell death^{28; 35}. The inhibition of Top1 results in the accumulation of DNA SSBs, while the inhibition of Top2 leads to the accumulation of DNA DSBs²⁵. The persistence of these breaks can activate DDR pathways and induce cell cycle arrest, senescence, or programmed cell death (apoptosis). Topoisomerase inhibitors are valuable tools in

both clinical and research settings. Although they have proven effective in the treatment of various cancers and infectious diseases, their use is not without limitations. Some topoisomerase inhibitors can cause toxic side effects such as cardiotoxicity or myelosuppression. Moreover, the emergence of drug resistance poses a challenge in the clinical management of diseases^{5; 36; 37}. Inhibition of Top2 via stalling the cleavage complex has been targeted with Top2 poisons as a mechanism of inducing cell death for chemotherapeutic applications for approximately 50% of cancer treatment plans. Non-covalent Top2 poisons used in cancer treatment include etoposide and doxorubicin. Etoposide and doxorubicin are polyphenolic compounds that stall the Top2 cleavage complex resulting in unresolved DSBs in a dose-dependent manner and promote cell death^{5; 36; 37}. However, some cells may use illegitimate DNA repair pathways that can promote genetic rearrangements. Approximately 5% of patients who receive etoposide as a chemotherapeutic for one cancer develop secondary leukemia characterized by chromosomal translocations between 11q23 and the *MLL* gene locus and several partner genes including *AF4*, *AF9*, *ELL*, and *ENL* are associated with the development of aggressive mixed-lineage leukemias. These leukemias are particularly rapid in progression and have poor prognoses in infants. *MLL* rearrangements can result in acute myeloid leukemias (AML) or acute lymphoblastic leukemia (ALL) diagnoses with preferential partner genes for rearrangements. AML typically partners with *AF9* or *AF10*, whereas ALL typically partners with *AF4*³⁸. *MLL* and *AF9* contain breakpoint cluster regions with several Top2 cleavage sites³⁹.

1.5 Natural Compounds, Bioflavonoids, and their ability to disrupt Top2.

Genistein is a bioflavonoid and belongs to a subgroup of bioflavonoids, isoflavones, naturally occurring in plants, fruits, vegetables, tea, cocoa, and wine⁴⁰. In adults, bioflavonoids have cardioprotective, cytoprotective, chemoprotective, antioxidant, and anti-inflammatory properties⁴⁰⁻⁴². Bioflavonoids' proposed health benefits have subjected them to further use in energy drinks and supplements⁴³⁻⁴⁸. The Food and Drug Administration approved a health claim for soy protein. This

claim described 25 grams of soy protein per day could potentially reduce the risk for cardiac disease if accompanied by a reduced cholesterol and saturated fat diet. Further, isoflavones were originally studied because populations that have a high concentration of soy in their diet have reduced rates of osteoporosis, heart disease, and uterine cancers, as well as other hormone-associated cancers.

Isoflavones potentially influence hormone cancers because of their ability to act as phytoestrogens. Phytoestrogens, plant estrogen-like compounds, are capable of interacting with human estrogen receptors because of their analogous structure to 17 β -estradiol. Because of this activity, genistein can inhibit metastasis, and has a potential application for easing menopausal symptoms, which is particularly beneficial for individuals seeking to avoid artificial hormone therapies⁴⁹. Further, genistein supplementation has been associated with endocrine disruption in developing rodents, with potential implications for negatively impacting spermatocytes, their production, and the development of the reproductive system in males⁵⁰.

Genistein is also a polyphenolic compound resulting in biochemical similarities to etoposide and doxorubicin. Studies have demonstrated that genistein inhibits Top2 in a dose-dependent manner. (In cell culture models exposure to genistein can induce cleavage at the MLL gene locus and promote translocations between the *MLL* and *AF9* breakpoint cluster regions analogous to those observed in secondary and infant leukemias. There is epidemiological evidence that maternal consumption of bioflavonoids poses a threat to the developing fetus genome^{41; 51-54}. Because genistein can cross the placental barrier, it can influence the developing fetal genome⁵⁵. The fetal genome may be particularly prone to recombination events because it is highly proliferative and sensitive to environmental and endogenous toxins. Fetal genome stability has also been cited as influenced by maternal diet^{56; 57}.

Previous work has evaluated the impact of genistein *in vivo* to influence development in mammalian models through multiple methods of delivery (Table 1)⁵⁸⁻⁶². In these studies the supplemental genistein doses ranged from 2mg/kg-400mg/kg of genistein per day. One particular study in C57BL6 mice used doses 100, 500, 1000, 1500, and 2000ppm of genistein for 28 days. These doses were noted to replicate the peak serum concentrations of total genistein concentrations that are representative of humans who consume high levels of genistein and infants consuming soy formula⁶⁰. Other work mimics the human consumption of bioflavonoids with ranges of doses from 25 to 500mg/kg/day^{59; 60; 62} set to account for fluctuations in diet. The exact consumption of genistein is variable based on diet type and regional differences related to soy accessibility, but plant-based food sales in the United States have increased by 43% from 2019-2021⁴⁹. Other work outlines the consumption of dietary phenols by humans in the United States to be 884.1 mg per 1,000kcal/day on average from 2013-2016⁶³, and from 65 to 250mg/day⁴⁴. *In vivo* genistein has been evaluated for its potential to cause DNA damage in mice and rats, and was associated with a dose-dependent increase of cells in S phase hypothesized to be associated with frozen Top2 cleavage complexes halting the cell cycle. Further, placental quality changes such as reduced placental and fetal size are observed in rats orally treated with genistein, and the process of fetal development includes a highly proliferative and progenitor environment.

1.6 Literature Review of Genistein Research

Human exposure to genistein is mainly via eating plant-based protein alternatives and soy products. According to USDA's database for the isoflavone content of foods, many plant-based protein sources have high levels of isoflavones⁵⁸. Plant-based food sales in the United States have increased by 43% from 2019-2021⁴⁹. Another major source of genistein in humans is infant soy formula. The number of US infants who are fed soy formula each year is estimated to be 750000⁵⁹. The exact consumption of genistein is variable based on diet type and regional differences related to soy

accessibility. Studies have mimicked the human consumption of bioflavonoids with ranges of doses from 25 to 500mg/kg/day⁶⁰⁻⁶²

Previous work has evaluated genistein to influence development in mammalian models through multiple methods of delivery⁶⁰⁻⁶⁴. In these studies the supplemental genistein doses ranged from 2mg/kg-400mg/kg of genistein per day. One particular study in C57BL6 mice used doses 100, 500, 1000, 1500, and 2000ppm of genistein for 28 days. These doses were noted to replicate the peak serum concentrations of total genistein concentrations that are representative of humans who consume high levels of genistein and infants consuming soy formula as well as mimicking the serum concentrations found in the diet of an individual consuming high amounts of soy for health purposes⁶¹. Other work outlines the consumption of dietary phenols by humans in the United States to be 884.1 mg per 1,000kcal/day on average from 2013-2016⁶⁵, and from 65 to 250mg/day⁴⁴.

Previous research has also compared the levels of serum genistein in mice post-injection of 2mg/kg-200mg/kg of genistein to reported levels of serum genistein in soy formula-fed human infants. Mice injected with 8mg/kg per day of genistein showed serum genistein levels most comparable to soy formula-fed human infants at 0.5, 1, and 2 hours post-injection, however, levels were no longer comparable 6 hours post-injection. Genistein doses of 80mg/kg and 200mg/kg per day showed higher levels of absolute serum genistein in mice compared to soy-fed human infants up to 6 hours post-injection⁶⁶. It is important to note that similar genistein doses may result in different serum genistein levels based on the method of delivery. Since humans are most likely to be exposed to genistein orally, delivery by ingestion may be the most optimal way of replicating the effects of genistein in mice. Due to differences in how genistein is metabolized when administered orally versus when it is injected, serum genistein concentrations are much higher post-injection compared to post-ingestion of genistein^{66; 67}.

1.7 Hypothesis and Aims

DNA damaging agents induce DSBs that are repaired through NHEJ and HR. DSB-induced inter-chromosomal HR repair can lead to mutagenic events including the translocations associated with infant leukemia. I will use a unique Rainbow Mouse model developed in the Richardson lab to be the first direct demonstration of genistein diet supplementation to promote DSBs and promote DSB-induced inter-chromosomal HR *in vivo*.

AIM 1 – To evaluate genistein's capability of inducing inter-chromosomal HR in proliferative/filtering organs.

To evaluate the potential of genistein to cause DNA DSBs and promote inter-chromosomal HR *in vivo*, I will induce DSBs via genistein supplementation in Rainbow mice for 28 days, and evaluate the production of GFP⁺ inter-chromosomal HR recombinants in the other organs through fluorescent microscopy and flow cytometry. *I hypothesize that in liver, kidney and bone marrow, because these organs are highly proliferative and/or filtering in metabolism, there will be genistein-induced HR.*

AIM 2 – To evaluate genistein's capability of inducing inter-chromosomal HR *in-utero*.

I will induce DSBs via genistein supplementation in Rainbow female mice from prior to pregnancy through E13.5, and evaluate the production of GFP⁺ inter-chromosomal HR recombinants in mouse embryonic fibroblasts (MEFs) and fetal liver through flow cytometry and fluorescent microscopy. *I hypothesize that maternal genistein consumption will demonstrate the ability to promote inter-chromosomal HR because of the proliferative and progenitor nature of the developing fetus.*

AIM 3 – To evaluate genistein's capability of inducing inter-chromosomal HR in spermatocytes.

In spermatocytes, this HR could influence the fetal genome through an increase in unresolved DSBs, influencing the rate and efficacy of reciprocal meiotic recombination. Because of the obligatory HR required for successful meiosis, we can use this organ as a model for recombination

events. I will induce DSBs via genistein supplementation in Rainbow mice for 28 days, and evaluate the production of

GFP+ inter-chromosomal HR recombinants in the spermatocytes through fluorescent microscopy..

I hypothesize that in the testes, because these organs are highly proliferative and engage in meiotic recombination, there will be genistein-induced HR.

Overall, my project may provide important data describing how genistein ingestion and supplementation has the potential to impact genome stability in adults as well as the developing fetal genome. My results imply a more mutagenic role of genistein has previously been described and serves as important evidence that genistein supplementation should be moderated.

CHAPTER 2: Methodology and Materials

2.1 The Transgenic Rainbow Mouse Model to Study Inter-chromosomal HR

The Rainbow Mouse model is the first transgenic mouse model able to assess *in vivo* DNA DSB repair by inter-chromosomal HR. This model is composed of three major constructs (figure 4). The first construct, oGFP^s, is a non-functional GFP reporter mutated with the insertion of an I-SceI endonuclease recognition site and includes a downstream IRES-DsRed marker. The second construct, yGFP^s, is a non-functional GFP reporter mutated with the insertion of an I-SceI endonuclease recognition site and includes a downstream IRES-PhiYFP marker. The IRES-DsRED and IRES-phiYFP markers are expressed as indicators of a functional system in an open chromatin structure. The I-SceI mutations are in staggered locations on the yGFP^s and oGFP^s constructs maintaining a 650 base pair homology available for HR. If a DSB occurs in the vicinity of the GFP constructs and processing of the ends creates ssDNA tails within the GFP gene, then a homology search and interchromosomal HR repair can occur. With inter-chromosomal HR a functional GFP gene is created and GFP⁺ cells can be visualized using fluorescent microscopy techniques and FACS. As control for my studies, the Rainbow Mouse model also includes a third construct with the I-SceI endonuclease in a bi-cistronic TET-ON system with a constitutively expressed repressor rt-TAN. This repressor prevents the expression of the CMV promoter until interaction with doxycycline/tetracycline which then allows for the expression of I-SceI that creates site-direct DSBs in both the yGFP^s/oGFP^s constructs thus readily facilitating DSB induced inter-chromosomal HR.

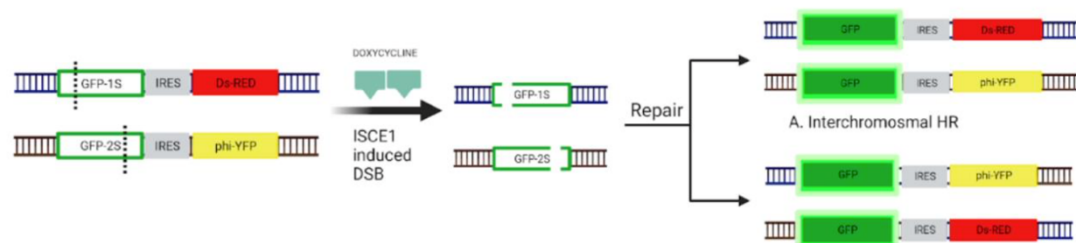


Figure 4: The Rainbow mouse model constructs outlining the induction of DNA DSBs via I-SceI.

2.2 Embryonic Stem Cell Culture and Genistein Treatment

The mouse stem cell line C2 were treated in 75 μ M, 100 μ M, and 150 μ M genistein in DMSO solution respectively for three hours at 37 degrees Celsius and 5% CO₂. The cells were then spun at 1000 RPM for 10 minutes. The supernatant containing the genistein solution was removed, and cells were plated at 5×10^6 per 10cm plate with fresh ES media, and incubated for 24 hours at 37 degrees Celsius and 5% CO₂. Cells were then placed in media containing 200 μ g/ml G418, and imaged 10 days later using an inverted microscope.

2.3 PCR and Genotyping

Mice were ear punched using 2mm punching scissors. The punches were placed into individual 1.5ml labeled microcentrifuge tubes. Then, the punches were placed into labeled 200 μ l PCR tubes. The KAPA genotyping kit was used to isolate DNA from the punches. 88 μ l of Milli-Q water, 1X buffer, and 20mU of enzyme were added to each punch.. Following DNA isolation and amplification protocol the tubes were spun using the mini-mouse centrifuge for 1 minute. The supernatant was transferred into new 1.5 ml tubes for storage.

PCR was formed with the following reagents in each reaction: 3 μ l forward primer, 3 μ l reverse primer, 5 μ l DNA at 1ug/ μ l, 14 μ l Milli-Q water, KAPA Hi-Fi PCR bead. A quick spin using mini centrifuge was performed to mix the components. The PCR program was utilized based on the transgene with the respective primer sequences: yGFP^s; Forward: 5' agttcatctgcaccaccgg 3', Reverse: 5' ggtaggtcttgcggcaatc 3', and amplifying the yfp at 51°C for 35 cycles; oGFP^s; Forward: 5' gctccaaggtgtacgtgaag 3', Reverse: 5' agcttgagtgccacgtagta 3', and amplifying the DsRed at 52°C for 30 cycles; I-Sce: Forward: 5' tcagcagtttagagttcggac 3', Reverse: 5' gatgtctctggcatactggt 3', and amplifying the I-Sce1 at 51°C for 35 cycles. Gel electrophoresis was performed following the PCR

with a 3% agarose gel. 4 μ l of loading dye was added to each sample for loading the gel, and the NEB 50bp ladder was used as a marker.

2.4 Primary MEFs Culture and Treatment

A mouse at E13-14 was euthanized via the IACUC protocol. Under the hood, the mouse was opened, the fetuses were extracted in a 10 cm plate with PBS. Each fetus was removed from their embryonic sac and decapitated. The heads were saved for DNA extraction and subsequent PCR. The remaining tissue was placed into a 6-cell well plate with 3 ml of trypsin. Tweezers and scissors were used to make a single cell suspension. This was repeated for all the fetuses. The tissue was incubated at 37 degrees and 5.0% CO₂ for 10 mins. 3 ml of MEF media (500ml DMEM, 70ml of FBS, 5ml of NEA, 5ml of L glutamine) was added to each well. Mix well. Use 5ml syringe and 22 gauge needle to make single cell suspension and remove clumps. Put the suspension in 15 ml tubes. Spin at 1000 rpm for 10 minutes. Remove supernatant and add 2 ml of fresh MEF media to the pellets. Plate on 10 cm plates, keeping individual samples separate. Add another 6 ml MEF media. Media was changed 24 hours later. The MEFs were plated to 1x10⁶ cells on a 10cm plate, treated with 100 μ M Genistein in culture medium for one hour at 37°C 5% CO₂, and photographed three days post treatment using fluorescent microscopy at an objective of 20x.

DNA isolation was performed from the heads. 950 μ l of DNA-PK buffer was added to the heads and 50 μ l of proteinase K. They were mixed well and incubated at 50 degrees overnight. The solution was mixed well to dissolve chunks and 1 ml phenol was added. Tubes were shaken 4-5 times by inverting. Samples were centrifuged at 12000 rpm for 10 minutes. The supernatant was removed and placed in a new tube. The addition of phenol and supernatant transfer was repeated. 1 ml of Phenol: chloroform: IIA was added to the supernatant in a new tube. Samples were shaken hard so the solution is hazy, and centrifuged at 12000 rpm for 10 minutes. The supernatant was removed

and placed in a new tube. 100 μ l of 3M sodium acetate and twice the total volume of 100% ETOH was added. Samples were mixed well to visualize the DNA. Samples were centrifuged at 12000 rpm for 10 minutes. The supernatant was removed, and 100 μ l of cold 80% ethanol was added to the white pellet. Samples were centrifuged at 12000 rpm for 10 minutes. The supernatant was removed, and the pellet was air dried for 15-20 minutes. Samples were dissolved in the desired amount of storage buffer (TE ranging from 200-350 μ l). PCR protocol was followed as described above.

2.5 Genistin Treatment Protocol

Adult mice were trained to eat genistin powder mixed into Nutella. The training period included housing mice in groups, and introducing 0.5mg of Nutella on a dish while removing chow until the Nutella is finished. This is repeated for three days. On day four and five the mice are separated and provided 0.35mg of Nutella on a dish in a new cage without chow to mimic the experimental conditions. Following day 5 the experiment is started, and mice receive individual doses, in separate cages, of 250mg/kg of genistin mixed into approximately 0.35 mg of Nutella. The amount of Nutella was adjusted to the amount of genistin to mask the bitterness of the compound. In periods of time where the mice have an adverse response to the bitter flavor of the genistin doses were provided in smaller amounts throughout the day to ensure their complete dose was received. Adult mice received genistin at 250 mg/kg/day for 28 days and euthanized at day 28. Pregnant females were trained to eat the Nutella before mating and fed genistin from E0 (conception) to E13.5, and euthanized at E13.5. Visualization of plugs was used to track fertilization and conception dates.

2.6 Mouse Perfusion

Mice were placed under anesthesia following the IACUC standard operating procedure for the anesthetic machine. The mouse was placed into the induction chamber in the biosafety cabinet for

the induction of anesthesia. The vaporizer was turned to a concentration of 3.5 – 4.0% by pushing down on the little black button and turning the knob in a counter-clockwise direction. Oxygen was introduced at this time by turning the green knob in a counter-clockwise direction to 1.0-2.0 liters. Once the animal has lost its righting reflex (ability to stay sternal), the animal was removed from the induction chamber and placed into a nose cone, which covers the rodent's nose and head. The mouse will relax and become immobile, but at this depth of anesthesia they can easily be aroused by painful stimuli. Adequate time, approximately 5-10 minutes must be provided so the anesthesia can deepen until such responses to pain are absent. Check the pain response with the pinch test but pinching each limb with tweezers. After the correct depth of anesthesia is achieved, the Isoflurane should be turned down to a concentration of 1.5 - 2.0%. Oxygen was turned down to 0.6 liters. Whole tissue perfusion was performed via intracardiac injection of 20 mls 1x PBS with a syringe, followed by 10mls of 4% paraformaldehyde (PFA). Secondary euthanasia was performed via cervical dislocation post organ removal.

2.7 Organ Isolation and Fixation for FACS

The mice, treated with 28 days of genistein at 250mg/kg, were euthanized according to IACUC protocols via CO₂ chamber and secondary cervical dislocation. The liver, both femurs, both kidneys, and both testes were extracted. One kidney, testes, and liver lobe were set aside for cryo-sectioning. The other organs were homogenized. Using a mortar and pestle filter, the tissues were ground into a single cell suspension. For bone marrow, the femur was open from both ends of the bone with scissors. A 3 ml syringe and attached 22g needle was filled with 2ml of PBS and inserted into one end of the bone. The PBS was used to flush the bone marrow out into a 6 well plate. The bone marrow was homogenized via needle and syringe. The single cell suspensions in PBS were then spun at 1000 RPM for 10 minutes. From here, the pellets were resuspended in 4% PFA and set to incubate protected from light for 20 minutes at 4 degrees Celsius. The cells were centrifuged at 1000 RPM for ten minutes, and the supernatant was discarded. The cells were washed with 1 ml

of 1x PBS three times before resuspension in 1ml of FACS buffer. The cells were counted and divided among FACS tubes as needed for analysis. This process was repeated for in-utero analysis of fetal tissues. A pregnant mouse of day E13.5 was euthanized via IACUC protocols. The fetuses were removed from the uterus and decapitated for DNA isolation as described under the MEFs protocol. The fetal liver, whole fetal tissue, and placentas were isolated and homogenized for FACS following the protocol described above.

2.8 Organ Isolation and Fixation for ImageStream X Analysis

One million cells were isolated from the samples prepared for FACS and centrifuged at 1000 RPM for 10 minutes. The supernatant was removed, and the cells were resuspended in 200ul of PBS. A 1:1000 dilution of DAPI was added to the cells, which incubated for 5 minutes protected from light. Cells were centrifuged at 1000 RPM for 10 minutes. The supernatant was removed, and the cells were resuspended in 200 μ l of PBS, and analyzed via the ImageStream X.

2.9 Hoechst Staining

Placed one decapsulated testis in a 15-ml tube. Added 3-ml of Gey's Balance Salt Solution (GBSS) containing 120 U/ml of Collagenase type I. Added 10 μ l of DNase I (1mg/ml stock solution in 50% glycerol) and shook it vigorously by hand until testicular tubules start to dissociate. Agitated horizontally at a maximum of 120 rpm for 15 min at 33°C. Centrifuged for 10 minutes at 1000 RPM at room temperature, and discarded supernatant. Added 3-ml of Gey's Balance Salt Solution (GBSS) containing 120 U/ml of Collagenase type I. Added 10 μ l of DNase I (1mg/ml stock solution in 50% glycerol) and shook it vigorously by hand until testicular tubules start to dissociate. Agitated horizontally at a maximum of 120 rpm for 15 min at 33°C. Centrifuged for 10 minutes at 1000 RPM at room temperature, and discarded supernatant. Added 2.5 ml of GBSS containing Collagenase type I, 50 μ l of trypsin, and 10 μ l of DNase I (1mg/ml), and inverted the tube several times. Agitated horizontally at a maximum of 120 rpm for 15 min at 33°C. Used a plastic disposable

Pasteur pipet with wide orifice to pipette gently up and down for 3 min until no clumps remain. Added 30 μ l of trypsin, 10 μ l of DNase I, 40 μ l of Hoechst 33342 resuspended in DMSO (10 mg/ml), and inverted the tube several times. Agitated horizontally at a maximum of 120 rpm for 15 min at 33°C. Added 400- μ l of fetal calf serum (FCS) and mixed by inverting to inactivate trypsin. Final staining is performed by adding 50 μ l of Hoechst 33342 resuspended in DMSO (10 mg/ml), and 10 μ l of DNase I (1 mg/ml). Agitated horizontally at a maximum of 120 rpm for 15 min at 33°C. The dissociated testis sample is then passed through 50 μ m mesh, then 5 μ l of propidium iodide (PI) solution is added and sample is gently mixed by pipetting several times with disposable Pasteur pipette. Sample was transferred to a 5-ml plastic FACS tube and stored at 4 degrees Celsius and protected from light until FACS analysis using the ARIA Flow cytometer.

2.10 Embedding and Cryosectioning

The testes, kidney, uterus, and liver were extracted and placed into 4% paraformaldehyde for 24 hours. The organs were moved to 30% sucrose for 24 hours. The organs were briefly dried on a paper towel before flash freezing and embedding into a block of OCT. Embedding and flash freezing was performed simultaneously using rapid freeze sprayed into an Erlenmeyer flask (to prevent evaporation). The rapid freeze was then poured in a base chamber resting on top of lab armor metallic alloy beads (to keep the chamber cold for flash freezing) and surrounding the disposable embedding blocks. The bottom of the disposable embedding blocks was filled with optimal cutting temperature (OCT) compound and began to freeze. After the edges of the block began to freeze the individual organ was suspended in the OCT. The testis was embedded in a “longitudinal” position, horizontal with the epididymis positioned dorsally until it was held upright by the OCT. The kidney was embedded horizontally to allow for visualization of the medulla and resulted in a semi-circle section of the face of the kidney. One small lobe of the liver was embedded vertically; liver tissue is homogenous and does not require specific orientation for this protocol. OCT was added to cover the top of the block and allowed to freeze. Here, the blocks were removed

from the rapid freeze, left in the molds, and covered in aluminum foil. They can be stored at -80 degrees Celsius or sectioned immediately. If storing at -80, thaw to -20 before sectioning. Sectioning was performed using the cryostat. All organs were sectioned at 6um, using charged tissue slides, and stored at -20 degrees until staining.

2.11 Hematoxylin and Eosin Staining

Kidney: Slides were exposed to the following sequence of reagents: DI Water, 1 minute; DI Water, 1 minute; Hematoxylin, 15 seconds; Running tap water, until the water runs clear; DI Water, 2 minutes; 95% alcohol, 30 seconds; Eosin, 15 seconds; 95% alcohol, 30 seconds; 95% alcohol, 30 seconds; 100% alcohol, 1 minute; 100% alcohol, 1 minute; Xylene, 2 minutes; Xylene, 1 minute; Xylene, 1 minute. Slides were then cover-slipped with Cytoseal mounting agent and set to dry on the countertop for 3 hours before imaging with the EVOS m5000.

Liver: Slides were exposed to the following sequence of reagents: DI Water, 1 minute; DI Water, 1 minute; Hematoxylin, 15 seconds; Running tap water, until the water runs clear; DI Water, 2 minutes; 95% alcohol, 30 seconds; Eosin, 25 seconds; 95% alcohol, 30 seconds; 95% alcohol, 30 seconds; 100% alcohol, 1 minute; 100% alcohol, 1 minute; Xylene, 2 minutes; Xylene, 1 minute; Xylene, 1 minute. Slides were then cover-slipped with Cytoseal mounting agent and set to dry on the countertop for 3 hours before imaging with the EVOS m5000.

Testes: Slides were exposed to the following sequence of reagents: DI Water, 1 minute; DI Water, 1 minute; Hematoxylin, 25 seconds; Running tap water, until the water runs clear; DI Water, 2 minutes; 95% alcohol, 30 seconds; Eosin, 15 seconds; 95% alcohol, 30 seconds; 95% alcohol, 30 seconds; 100% alcohol, 1 minute; 100% alcohol, 1 minute; Xylene, 2 minutes; Xylene, 1 minute; Xylene, 1 minute. Slides were then cover-slipped with Cytoseal mounting agent and set to dry on the countertop for 3 hours before imaging with the EVOS m5000.

Uterus: Slides were exposed to the following sequence of reagents: DI Water, 1 minute; DI Water, 1 minute; Hematoxylin, 15 seconds; Running tap water, until the water runs clear; DI Water, 2 minutes; 95% alcohol, 30 seconds; Eosin, 15 seconds; 95% alcohol, 30 seconds; 95% alcohol, 30 seconds; 100% alcohol, 1 minute; 100% alcohol, 1 minute; Xylene, 2 minutes; Xylene, 1 minute; Xylene, 1 minute. Slides were then cover-slipped with Cytoseal mounting agent and set to dry on the countertop for 3 hours before imaging with the EVOS m5000.

2.12 Immunohistochemistry

Slides were removed from the freezer and warmed to room temperature (approximately 10 minutes on the bench top). The slides were washed slide twice with PBS. A circle was drawn on the slide around the tissue with a hydrophobic barrier pen. The slides were washed twice for 10 minutes with 1% animal serum in PBS-T. Then, blocked for non-specific binding by incubating the tissue sections with 5% serum in PBS-T for 30 minutes at room temperature. The primary antibody RAD51 (Catalog # MA1-23271) was diluted in blocking buffer at a ratio of 1:50 (antibody:5% animal serum in PBS-T) and then added to the sections. These slides were incubated at room temperature for 1.5 hours in a dark, moist box. The incubation was continued overnight at 4°C in the dark, moist box. The, the sections were washed twice with 1% serum PBS-T for 10 minutes each. The fluorescent label conjugated secondary antibody was diluted in blocking buffer at a ratio of 1:50 (antibody:buffer) and added to the sections (Alexfluor 750 (Invitrogen, catalog # A-21037), Alexafluor 405(Invitrogen, catalog # A-31553)). Samples were incubated at room temperature for 1.5 hours in a dark moist box. The sections were washed twice with 1% serum PBS-T for 10 minutes each. The excess liquid was tapped off. One drop of prolong antifade (gold or diamond) mounting medium was added to the slide, and then a coverslip was placed over the tissue sections. These were incubated at room temperature, protected from light, for 24 hours. Slides were

examined under the EVOS m5000. Slides can be stored between -20°C and 4°C in a dark slide box or slide book.

CHAPTER 3: Results

3.1 Validation of Rainbow Mouse Model and DSB-induced Inter-chromosomal HR

Rainbow mouse model mice were generated by crossing single homozygous yGFP^s and oGFP^s mice (described in Methods) to result in heterozygous yGFP^s/oGFP^s mice for studies on genistein diet supplementation. We confirmed the presence of both the yGFP^s and oGFP^s nonfunctional reporter constructs by PCR. Figure shows the presence bands yGFP^s 318bp and oGFP^s 447bp, respectively. For comparison against endonuclease targeted DSBs and repair, homozygous yGFP^s/oGFP^s mice were crossed with the I-SceI inducible mice (K Lalwani and C Richardson, unpublished).

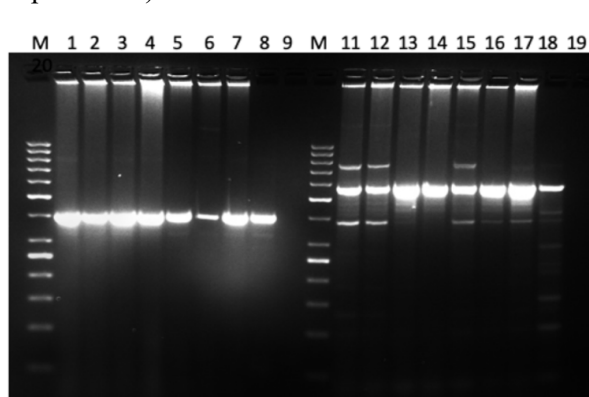


Figure 5. Confirmatory PCR showing the presence of yGFP^s and oGFP^s nonfunctional reporter constructs in MEFs. Lanes are as follows: NEB 50bp ladder, MEFs oGFP^s 2-7, positive control, negative control, NEB 50bp ladder, MEFs yGFP^s 11-17, positive control, negative control.

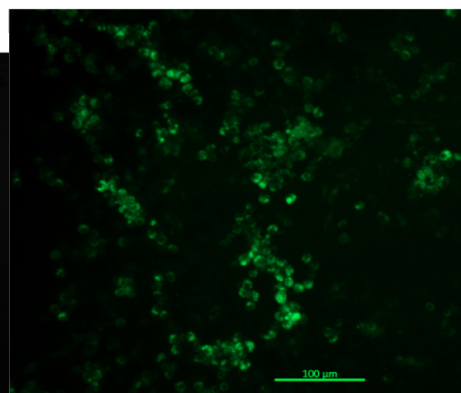


Figure 6. GFP+ mouse embryonic fibroblasts (MEFs) derived from the Rainbow mice. The MEFs were plated to 1×10^6 cells on a 10cm plate, treated with 100M genistein in culture medium for one hour at 37°C 5% CO₂, and photographed three days post treatment using fluorescent microscopy at an objective of 20x.

Mouse embryonic fibroblasts (MEFs) were isolated. PCR of DNA extracted from MEFs (lanes 1-7 and 11-17 of figure 5) confirmed the presence of the both the yGFP^s and oGFP^s nonfunctional reporter constructs. To demonstrate the potential for genistein to induce inter-chromosomal HR events in cultured cells derived from the Rainbow mice, cultured MEFs were treated with 100 μM Genistein for one hour. Cells were then allowed to recover and DSB repair to occur. Cells were analyzed three days post treatment using fluorescent microscopy (20x). GFP+ cells were

readily detectable, supporting the hypothesis that genistein is capable of inducing generalized DSBs and inter-chromosomal HR repair events *in vitro* (Figure 6).

3.2 Induction of Inter-chromosomal HR in Proliferative and Filtering Organs by Genistein

Kidney: Following 28 days of genistein 250mg/kg/day ingestion, tissue sections from kidneys were used for fluorescence IHC (figure 7). Morphological analysis of the kidneys did not reveal any structures different from wild-type or untreated mice. GFP expression was observed in both the 250mg/kg/day genistein treated mice and the mice expressing the I-SceI endonuclease. In the genistein treated mice, GFP+ cells were localized to clusters each consistent with an individual inter-chromosomal HR event in one cell that locally proliferated. The cells expressing GFP were within the tubular epithelial structures directly associated with filtering and nephron function. In the I-SceI-expressing mice the GFP+ cells were more isolated and observed throughout the sections.

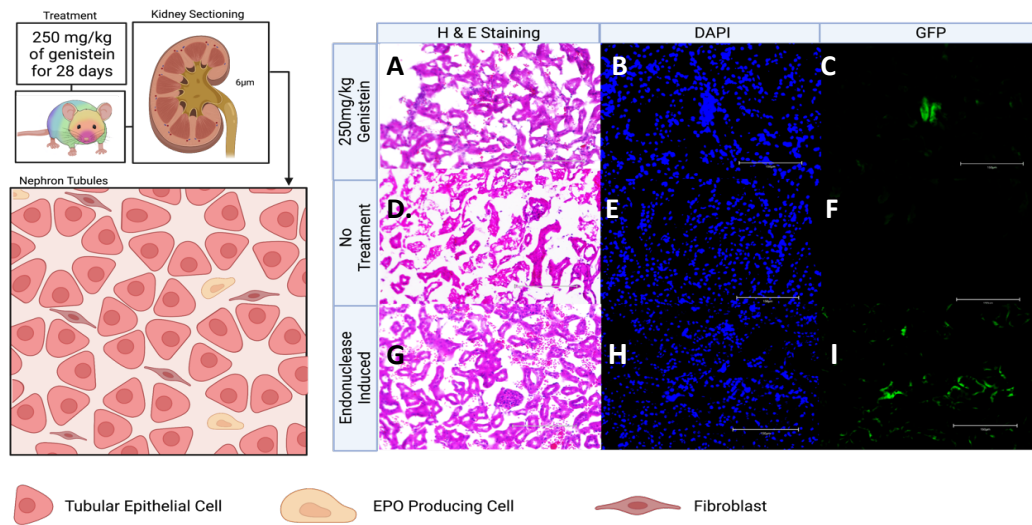


Figure 7. Rainbow mice were treated with 250mg/kg/day of genistein for 28 days and sections from their kidney were stained with hematoxylin, eosin and DAPI and scanned for GFP using the EVOS m5000 imaging system. Hematoxylin and eosin staining of kidney tissue sections from mice a. Treated with 250mg/kg/day genistein for 28 days, d. Exposed to no treatment, g. Induced with endonuclease. DAPI staining of liver tissue sections from mice b. Treated with 250mg/kg/day genistein for 28 days, e. Exposed to no treatment, h. Induced with endonuclease. GFP images of kidney tissue sections from mice c. Treated with 250mg/kg/day genistein for 28 days, f. Exposed to no treatment, i. Induced with endonuclease.

Single cell suspensions of total kidney cells were analyzed by flow cytometry (FACS) (figure 8). GFP+ recombinants resulting from inter-chromosomal HR were readily detectable in 4 of 5 mice for an overall average calculated relative maximum frequency of 4.1×10^{-6} . By contrast, no GFP+ cells were detected in wild type or untreated mice. These data support the hypothesis that *in vivo* exposure to genistein can promote inter-chromosomal HR events in the kidney.

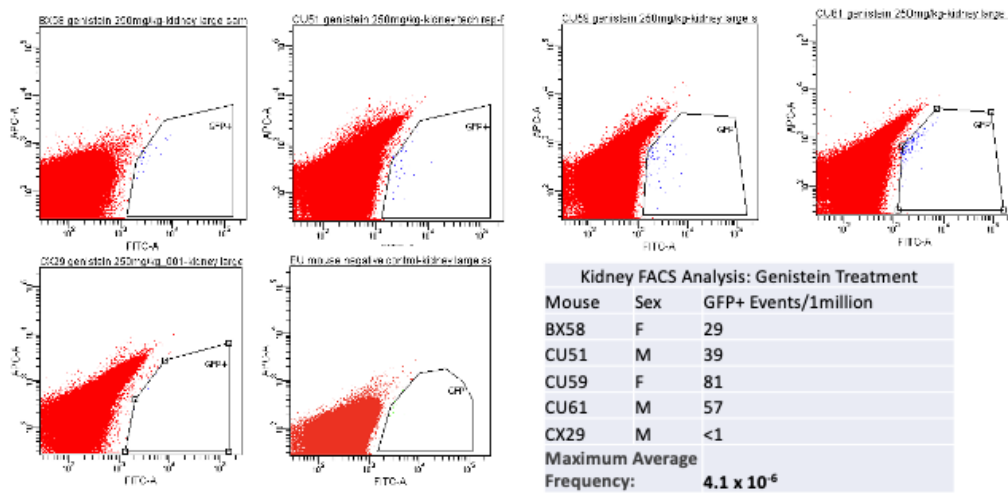


Figure 8. FACS analysis in the kidney of various genistein-treated mice. Table outlining the various mice used in the analysis, their sex, and the number of GFP+ cells in each mouse.

Liver: Following 28 days of genistein 250mg/kg/day ingestion, tissue sections from livers were used for fluorescence IHC (Figure 9). Morphological analysis from 4 of 5 mice did not reveal any structures different from wild-type or untreated mice. One mouse (female) presented with a clotted, dark and splotchy appearance to the liver that could be associated with an infection or old age. In all 5 genistein treated mice, no GFP+ cells were observed in liver sections, similar to those from untreated mice. However, our inducible system was able to produce GFP positive cells in small groups, which suggests possible clonal expansion.

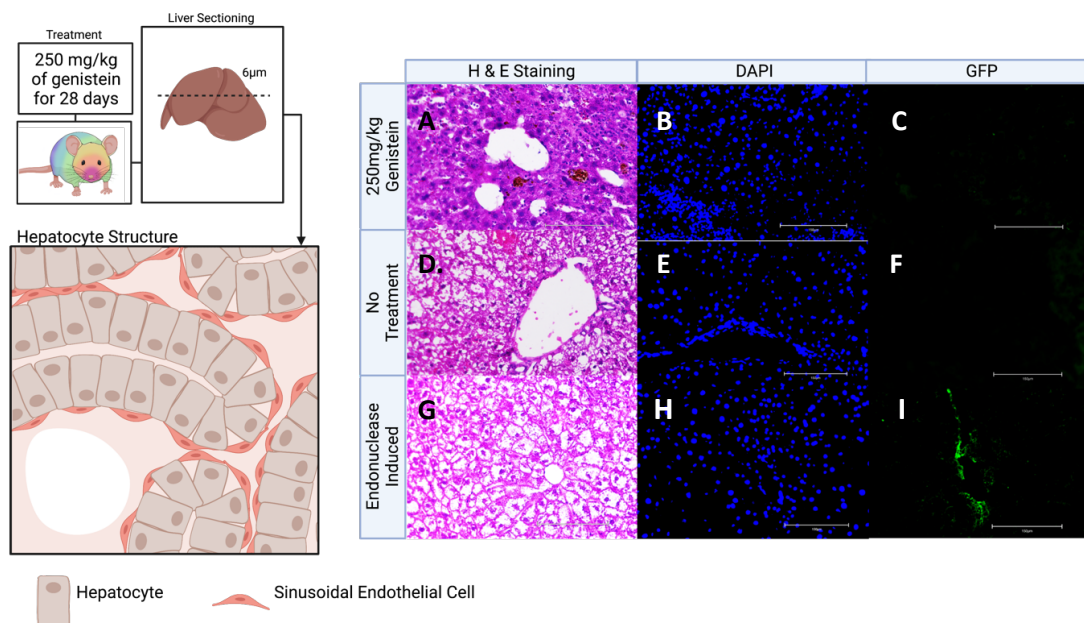


Figure 9. Rainbow mice were treated with 250mg/kg/day of genistein for 28 days and sections from their liver were stained with hematoxylin, eosin and DAPI and scanned for GFP using the EVOS m5000 imaging system. Hematoxylin and eosin staining of liver tissue sections from mice a. Treated with 250mg/kg/day genistein for 28 days, d. Exposed to no treatment, g. Induced with endonuclease. DAPI staining of liver tissue sections from mice b. Treated with 250mg/kg/day genistein for 28 days, e. Exposed to no treatment, h. Induced with endonuclease. GFP images of liver tissue sections from mice c. Treated with 250mg/kg/day genistein for 28 days, f. Exposed to no treatment, i. Induced with endonuclease.

In order to quantify the relative frequency of these events and possible capture rare events in a large sample size, single cell suspensions of total liver cells were analyzed by FACS (Figure 10). GFP+ recombinants resulting from inter-chromosomal HR were not detected in 4 of 5 mice (<1 per 5 million cells) and only 3 GFP+ events were observed in 1 mouse (sample size 5 million cells). This observation is not statistically significant above untreated mice, but if confirmed in future studies would be an overall average calculated relative maximum frequency of 1.2×10^{-7} . Overall, fluorescent microscopy and FACS indicated GFP+ events in the liver of our genistein-treated mice are extremely rare to undetectable.

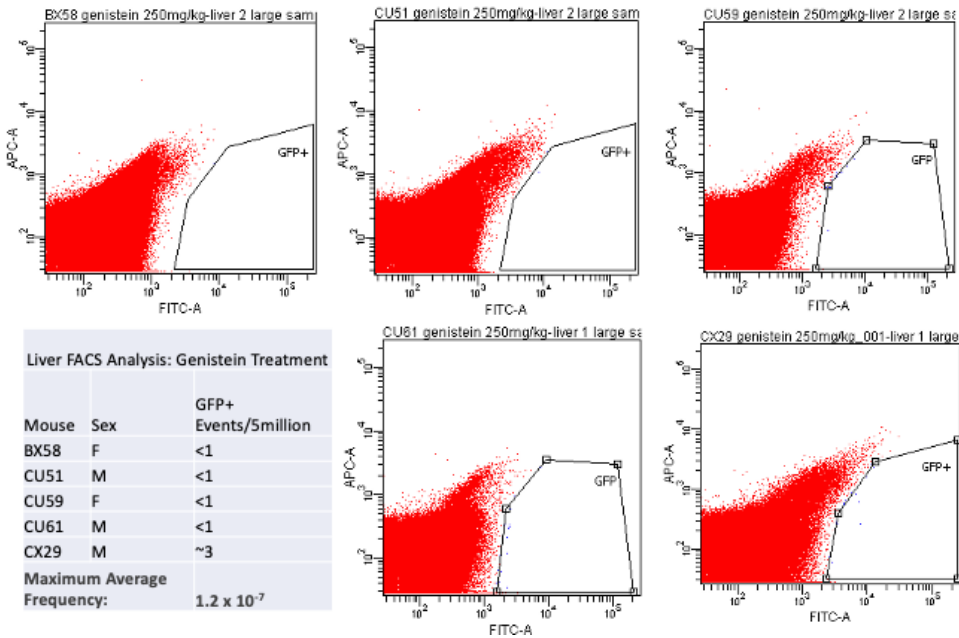


Figure 10. FACS analysis in the liver of various genistein-treated mice. Table outlining the various mice used in the analysis, their sex, and the number of GFP+ cells in each .mouse.

Bone Marrow: Following 28 days of genistein 250mg/kg/day ingestion, single cell suspensions of total bone marrow cells were analyzed by FACS (Figure 11). GFP+ recombinants resulting from inter-chromosomal HR were not detected in 2 of 5 mice (<1 per 2.5 million cells) and only a small number of GFP+ events were observed in the each of the other 3 mice (sample size 2.5 million cells) with an overall average calculated relative maximum frequency of 1.1×10^{-6} (t-test p value = 0.026). Overall, fluorescent microscopy and FACS indicated GFP+ events in the bone marrow of our genistein-treated mice rare events.

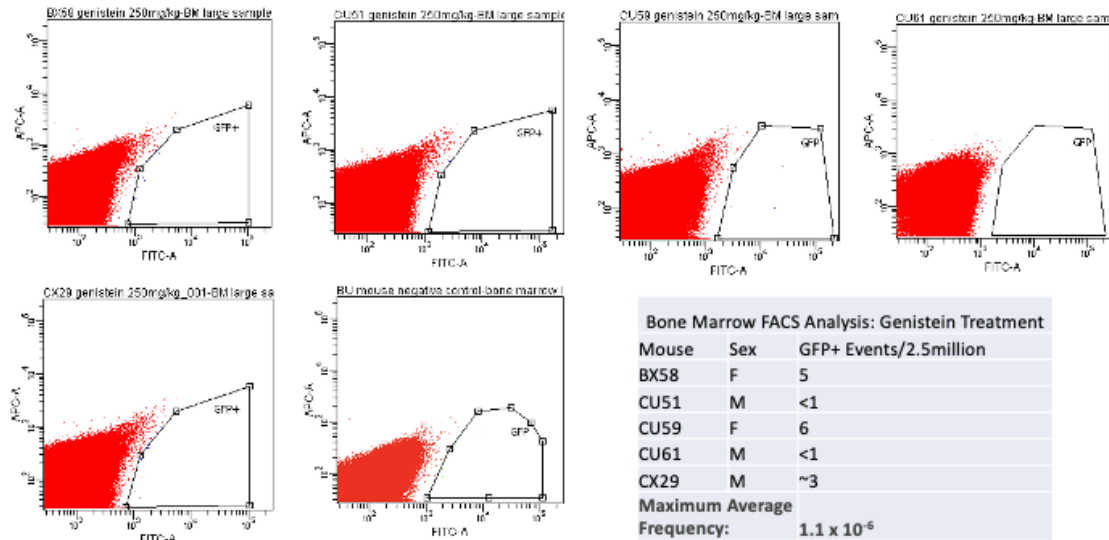


Figure 11. FACS analysis in the bone marrow of various genistein-treated mice. Table outlining the various mice used in the analysis, their sex, and the number of GFP+ cells in each mouse.

3.3 Induction of Inter-chromosomal HR in utero by Genistein

Female Rainbow mice were placed on genistein training, and full supplementation with genistein began the day of positive mating via plug identification. Pregnant females continued genistein supplementation until gestation day E 13.5. Whole fetal tissues were extracted and single cell suspensions analyzed by FACS (Figure 12). GFP+ cells resulting from inter-chromosomal HR were detectable in 2 of 3 fetuses. These data support the hypothesis that 250mk/kg/day genistein supplementation by a pregnant female can lead to inter-chromosomal HR recombination although the sample size is small.

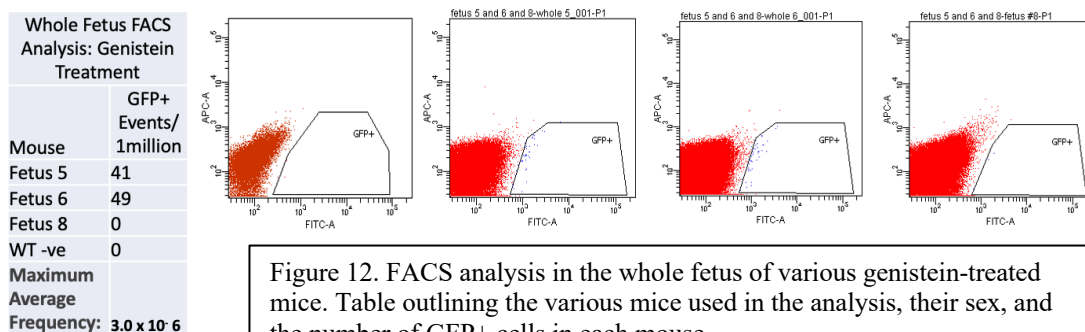


Figure 12. FACS analysis in the whole fetus of various genistein-treated mice. Table outlining the various mice used in the analysis, their sex, and the number of GFP+ cells in each mouse.

The fetal liver during mouse mid-gestation is the major organ for developing hematopoiesis. Therefore, to examine this specific sub-population, single cell suspensions from fetal livers were also isolated and examined by FACS (Figure 13). Fetus 5 and 6 each showed 1 GFP+ event and fetus 8 showed 7 GFP+ events per million (sample size 1 million cells). This observation is not statistically significant above untreated mice which consistently showed no GFP+ events, but if confirmed in future studies would be an overall average calculated relative maximum frequency of 3.0×10^{-6} . Overall, FACS indicated GFP+ events in the fetal liver of our genistein-treated fetuses are extremely rare or undetectable, similar to adult bone marrow and adult liver.

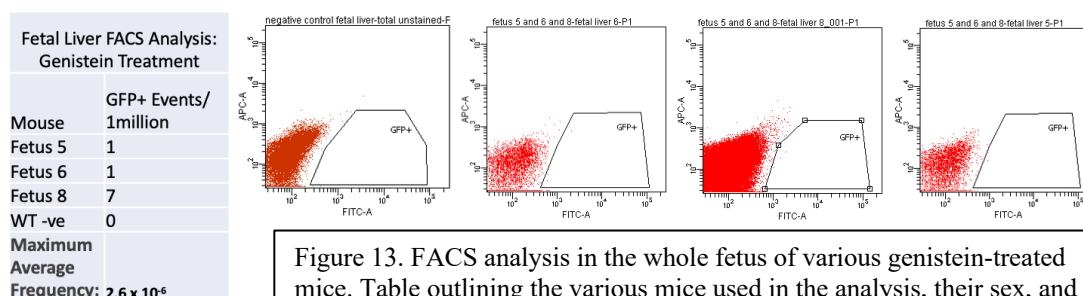


Figure 13. FACS analysis in the whole fetus of various genistein-treated mice. Table outlining the various mice used in the analysis, their sex, and the number of GFP+ cells in each mouse.

The placenta includes a mix of differing cell types including stem cells from the pregnant female to each individual fetus. Therefore, single cell suspensions of each placenta were analyzed by FACS (figure 14). GFP+ cells indicating inter-chromosomal HR were readily detectable in all three placenta samples for an overall average calculated relative maximum frequency of 2.6×10^{-6} . These detected GFP+ populations are larger than those observed in exclusively fetal tissues GFP producing tissues.

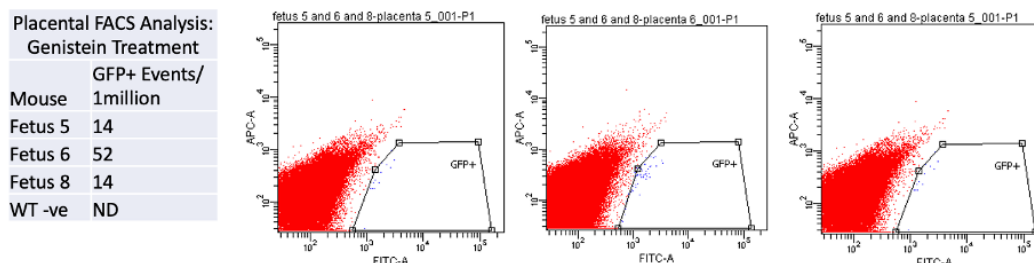


Figure 14. FACS analysis in the placenta of various genistein-treated mice. Table outlining the various mice used in the analysis, their sex, and the number of GFP+ cells in each mouse.

3.4 Induction of Inter-chromosomal HR in Reproductive Organs and Meiotic Tissue by Genistein

Testes: Following 28 days of genistein 250mg/kg/day ingestion, tissue sections from testes of 3 male mice were used for fluorescence IHC and FACS (figure 15). GFP+ cells resulting from inter-chromosomal HR were detectable in the testis; however all noted GFP+ cells were located outside of the testicular microtubules and not within the meiotic tubules. It was noted that 2 of 3 mice treated with genistein experienced enlarged gonads filled with a purulent-like substance. Both mice with enlarged gonads also had testicular wrinkling, which can be visualized in the peritubular structure in our H&E staining. Control endonuclease directed I-SceI mice did not present with any unique morphological changes to the testes or gonads. No GFP+ cells were detectable in untreated mice or mice with site directed I-SceI DSBs.. The lack of GFP in endonuclease-expressing mice suggests a possible mechanism for tolerance or preference for an apoptotic pathway in the meiotic cell types. Potentially, these inter-chromosomal HR events are occurring in cells associated with immune response or the endocrine system, rather than the spermatocytes within the microtubules.

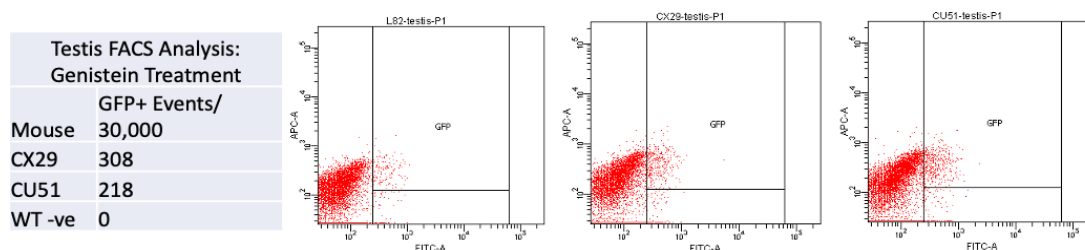


Figure 15. FACS analysis in the testis of various genistein-treated mice. a. Table outlining the various mice used in the analysis and the number of GFP+ cells in each mouse.

In the testes single cell suspensions of genistein treated mice GFP⁺ cells were readily detectable above background at a maximum calculated relative frequency of 8.7×10^{-3} (Figure 16). These data support the propensity for supplementary genistein to induce inter-chromosomal HR in the testes *in vivo*, and it is statistically significant at a p-value of 0.014 when compared to wild-type mice in an independent t-test of normalized data.

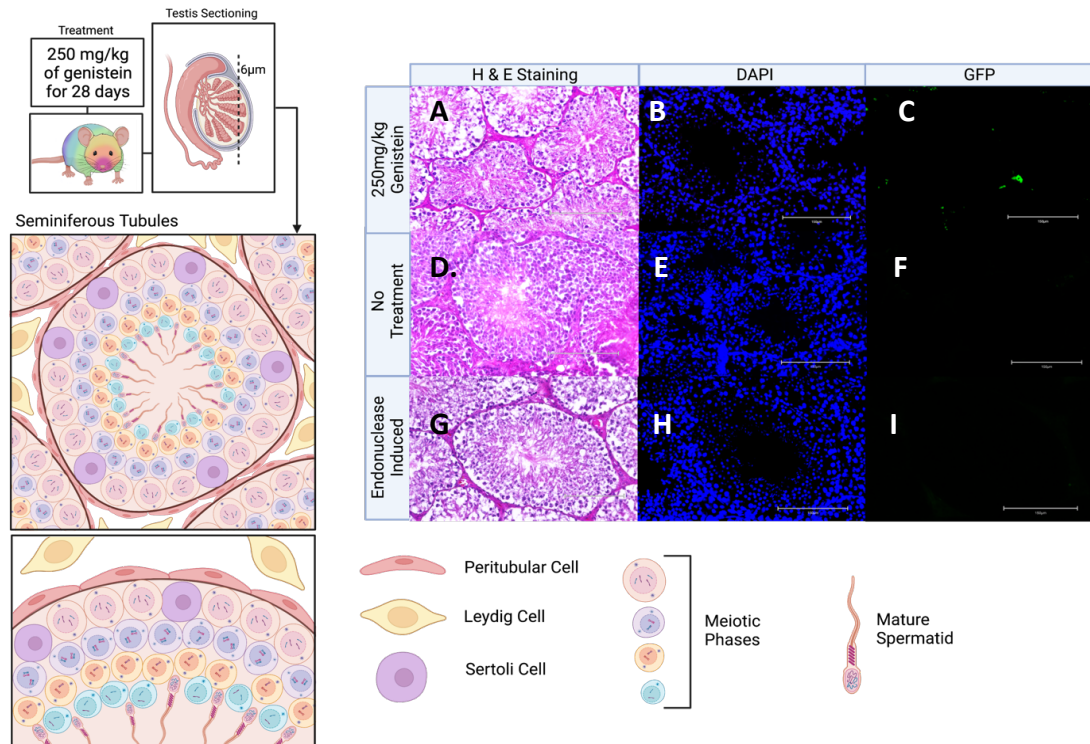


Figure 16. Rainbow mice were treated with 250mg/kg/day of genistein for 28 days and sections from their testes were stained with hematoxylin, eosin and DAPI and scanned for GFP using the EVOS m5000 imaging system. Hematoxylin and eosin staining of testis tissue sections from mice a. Treated with 250mg/kg/day genistein for 28 days, d. Exposed to no treatment, g. Induced with endonuclease. DAPI staining of testes tissue sections from mice b. Treated with 250mg/kg/day genistein for 28 days, e. Exposed to no treatment, h. Induced with endonuclease. GFP images of testes tissue sections from mice c. Treated with 250mg/kg/day genistein for 28 days, f. Exposed to no treatment, i. Induced with endonuclease.

Interestingly, our testes cells were expressing the essential recombination protein RAD51 within the inter-tubular space, which confirms we are experiencing homology search in HR between the seminiferous tubules of the testes. Our genistein treated mice produced GFP+ cells within the inter-tubular space and expressed RAD51. This further supports that genistein treatment *in vivo* can cause inter-chromosomal HR in the testes. Our I-Sce1 expressing tissues produced RAD51, as well as GFP+ cells, while our untreated group expressed RAD51, but did not present with any GFP as anticipated (Figure 17).

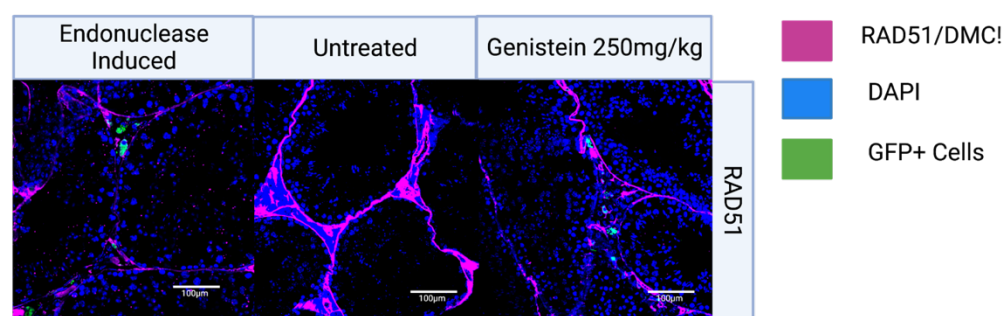


Figure 17. IHC of cryosectioned testis tissue of 6 μm imaged with confocal microscopy at an objective of 20x.

Uterus: Following 28 days of genistein 250mg/kg/day ingestion, tissue sections from ovaries of 2 male mice were used for fluorescence IHC and FACS (figure 17). GFP+ cells resulting from inter-chromosomal HR were detectable in the uterine tissue. One genistein treated mouse did present clotting in the fallopian tubes or potentially an infection of some kind; the exact cause of these morphological differences has not been determined, although it is clear there are excess red blood cells present. The genistein treated mice were producing GFP+ cells that appeared in smaller, isolated events between follicular columns, and occasionally in the epithelial cells lining

the follicular spaces. The Rainbow mice expressing I-Sce1 produced small regions of GFP clusters, which is potentially a clonally expanded group of proliferating cell types.

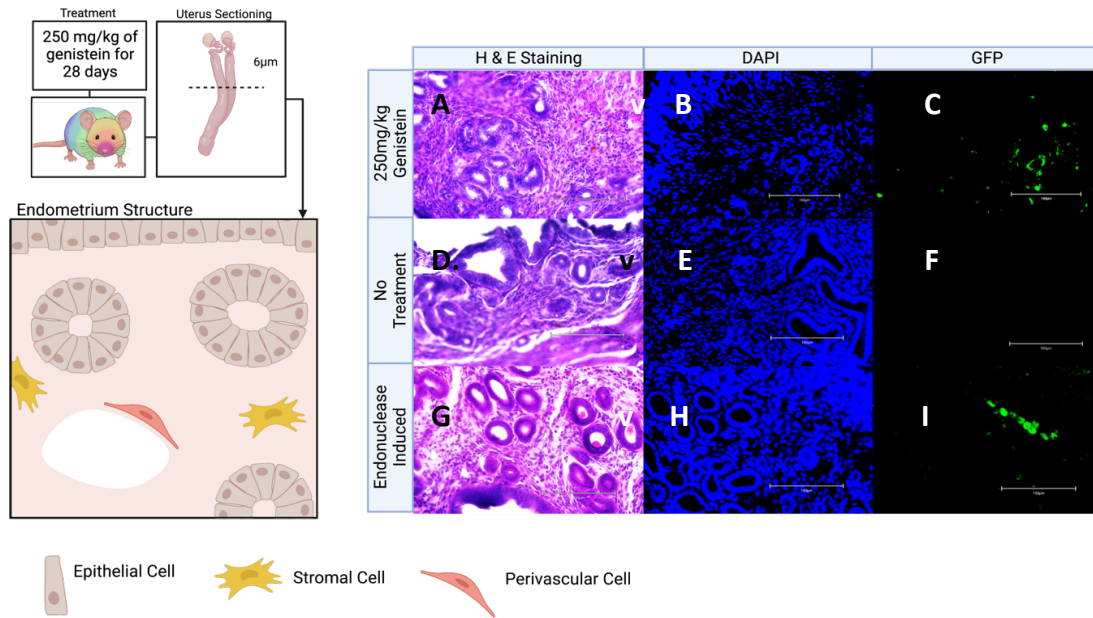


Figure 18. Rainbow mice were treated with 250mg/kg/day of genistein for 28 days and sections from their uterus were stained with hematoxylin, eosin and DAPI and scanned for GFP using the EVOS m5000 imaging system. Hematoxylin and eosin staining of uterine tissue sections from mice a. Treated with 250mg/kg/day genistein for 28 days, d. Exposed to no treatment, g. Induced with endonuclease. DAPI staining of uterine tissue sections from mice b. Treated with 250mg/kg/day genistein for 28 days, e. Exposed to no treatment, h. Induced with endonuclease. GFP images of uterine tissue sections from mice c. Treated with 250mg/kg/day genistein for 28 days, f. Exposed to no treatment, i. Induced with endonuclease.

CHAPTER 4: Discussion

In this project I have provided the first direct demonstration that genistein diet supplementation can promote *in vivo* inter-chromosomal HR events. These data have significant implications for diet-induced DNA damage, genome integrity, and chromosomal translocations associated with leukemias including infant leukemias.

4.1 Filtering and Proliferating Organs

In the kidney, GFP+ repair products resulting from inter-chromosomal HR were readily detectable. This supports our hypothesis that *in-vivo* exposure to genistein can cause inter-chromosomal HR in the kidney. The cells expressing GFP in the kidney were within the tubular epithelial structures directly associated with filtering and nephron function in the kidney (figure 7). These cells are considered slowly proliferative⁷⁰, and have been targeted in my work for their role in metabolism and filtering. Previously it has been shown that renal tubular epithelial cell dysfunction and cell death are acute kidney injury hallmarks, and these are important factors to consider when studying renal system function. These symptoms are often the products of significant stress on the kidney, and have been modeled with cisplatin-induced DNA damage. This work also elucidated homologous recombination as an important repair pathway for tubular repair⁷¹. Recurrent injury to these tubules is associated with the G2-M phase cell cycle arrest⁷⁰ and is it possible this arrest, induced by genistein in our work, is causing injury that is then repaired by homologous recombination in a mechanism similar to the proposed pathway in kidney organoids. Our dosing of 28 days may cause repeated kidney injury like the repeated injury modeled by cisplatin⁷⁰, and promote homology-directed repair⁷¹.

In our FACS analysis of the liver the average frequency of inter-chromosomal HR was 1.2×10^{-7} (figure 9). Large cell sample sizes were evaluated and support the conclusion events are rare or undetectable by FACS in the liver of genistein treated mice. In the liver there were not any significant morphological changes across most liver tissues (figure 9), evaluated via hematoxylin

and eosin staining, except for one female mouse who experienced a clotted, dark and splotchy appearance to the liver. The cause of this unique morphology is not completely clear, and could be associated with an infection or old age. Within our scanning for GFP no events were observed within the liver in our untreated and genistein groups. However, our inducible system was able to produce GFP positive cells in small groups. It is possible that although liver cells would be directly exposed to the topoisomerase II inhibition mechanism of genistein, the organ remains quite large and may be able to tolerate the genistein dose. Respectively, the mouse liver consumes a larger percentage of body weight than in humans or rats, and it is possible the larger concentration of hepatocytes is associated with stronger filtering and regenerative capabilities. The human liver maintains approximately 2% of total body weight, whereas the mouse liver is anywhere from 3-5% of the mouse's total body weight⁶⁸. Further, it is possible that apoptosis is the preferential pathway for managing topoisomerase II-inhibition for hepatocytes. Other work has evaluated flavonoids, specifically apple flavonoid-enriched fraction (AF4), and their influence on human hepatocellular carcinoma cells. It was found that treatment with AF4 inhibited cell growth in a dose dependent manner and induced apoptosis within 6 hours of treatment. Similar to genistein, AF4 induced G2/M phase arrest and functions as a topII inhibitor. These mechanistic similarities likely correlate with a shared preference for the apoptotic pathway over homologous recombination repair in hepatocytes but further analysis would be required to draw any relationship⁶⁹.

During FACS analysis of our genistein treated mice, we see that our mice are not readily producing GFP+ recombinants in the bone marrow. This observation is not statistically significant above untreated mice, but if confirmed in future studies would be an overall average calculated relative maximum frequency of 1.2×10^{-7} . These events are sporadic and unpredictable, and do not confer to a strong correlation between in-vivo genistein consumption and inter-chromosomal HR in bone marrow. This is an interesting juxtaposition to the prevalence of homologous recombination in normal B cell development. HR has an important role in B cell

development and promotes S-phase progression¹; however, we did not see significant prevalence of inter-chromosomal homologous recombination repair. It is possible that the cells are marked for apoptosis or that our dose is not acute enough to damage the bone marrow cells. Other work has implicated genistein in reducing bone loss rather than promoting DNA damage in bone marrow⁷²⁻⁷⁴. It is likely that etoposide, an intensive topoisomerase II inhibitor that my hypothesis is partially modeled on, is much more genotoxic and less tolerated by bone marrow cell types, as well²⁸. This suggests that at our dosing and treatment length, genistein is not causing many inter-chromosomal recombination events readily detectable by FACS, and those that have occurred are rare and sporadic. Confounding factors, like other mutations or more acute dosing, may be required to further destabilize the genome and lead to a significant frequency of inter-chromosomal HR repair.

4.2 In-utero

Genistein supplementation in-utero shows that inter-chromosomal HR events can occur, but sporadically, and may not affect every fetus. The placenta, isolated from fetuses treated with genistein from the date of conception through E13.5, was analyzed via FACS for GFP+ recombinants. It is possible that GFP+ recombinants are induced by supplementation of genistein throughout gestation, as these are larger populations of GFP+ cells than seen in other low GFP producing tissues, but a wild type control is required to draw any analysis or alternative hypotheses and normalize the data. It is possible that similar to the adult liver, apoptosis is a preferred pathway for flavonoid-induced DNA damage⁶⁹, but there is also recent work outlining the placenta as having a unique genetic landscape. It has been identified that in 1-2% of human pregnancies there are chromosomal aberrations that are confined to the placenta, and not within fetal cells. That study noted that fetal and placental lineages diverge spatially early on in embryogenesis, and that there was a high burden of somatic mutations in the placental samples they evaluated, counting 145 somatic substitutions. The authors also found that the presence of trisomy 10 had occurred in placental cells, but not in the fetus, and was deemed mosaic trisomic

rescue which supports their conclusion that the mechanisms that are working to protect the fetal genome are likely not operating in the same capacity in placental trophoblasts⁷⁵. I hypothesize a similar mechanism of genomic aberration tolerance could be occurring to allow inter-chromosomal HR in placenta, but largely not as prevalent in the whole fetus or fetal liver. Other work implicates genistein as reducing trophoblast populations⁷⁶, which is an interesting observation in conjunction with the discovery of a unique genetic landscape in the placenta particularly related to trophoblast populations⁷⁵.

Further, the fetal livers of fetuses isolated from genistein supplemented mothers from the date of conception to day E13.5 of gestation identified that events are very rare, and present similarly to the adult liver and bone marrow. It is apparent that genistein supplementation through day E13.5 of gestation does not readily cause inter-chromosomal HR in the fetal liver, and that the GFP+ cells may be the result of a rare event or background noise. If genistein is not readily inducing inter-chromosomal HR in bone marrow, it is understandable that the major source of hematopoietic cells during E13.5 is also not readily producing GFP+ cells.

4.3 Spermatocytes

Male Rainbow mice were treated with 250mg/kg/day genistein for 28 days, and it was observed that in our genistein treated mice there are populations of GFP at a maximum frequency of 8.7×10^{-3} . This data supports the propensity for supplementary genistein to induce inter-chromosomal HR in the testes *in vivo*, and it is statistically significant at a p-value of 0.014 when compared to wild-type mice in an independent t-test of normalized data. In our untreated mice there were no unique observations of organ anatomy and structure. Two of the three male mice treated with genistein experienced enlarged gonads filled with a purulent-like substance. Both mice with enlarged gonads also had testicular wrinkling, which can be visualized in the peritubular structure in our H&E staining. I-Sce1 endonuclease treated mice did not present with any unique morphological changes to the testes or gonads. GFP+ cells were not detected in

untreated mice, or in I-SceI mice. Although low in concentration, genistein supplemented mice did produce GFP⁺ cells in the testes, located outside of the testicular microtubules. Potentially, this inter-chromosomal HR are occurring in cells associated with immune response or the endocrine system, rather than the spermatocytes within the microtubules. The lack of GFP⁺ cells in our endonuclease-expressing mice suggests a possible mechanism for tolerance or preference for an apoptotic pathway in these cell types.

Our histological analysis of the testes introduces an interesting observation that the GFP⁺ cells, which I hypothesized would occur in spermatocytes, has not occurred in meiotic cells. Rather, it is likely the cells expressing GFP are Leydig cells. Because we are not seeing GFP⁺ recombinants in many bone marrow cells, I anticipate it is unlikely the GFP⁺ cells observed are derived from hematopoietic lineage. Further, genistein has been cited to interact with Leydig cells as a phytoestrogen. Due to the importance of Leydig cells for testosterone production, they have been studied in the context of phytoestrogens previously⁷⁷⁻⁷⁹. In rats, doses of 0, 5, 50, 500, and 1000 ppm of isoflavones was fed to the rats, and it was observed that there was a decrease of testosterone secretion associated with action from the phytoestrogens. This supports our observation of enlarged gonads in two of our three male mice treated with genistein. Due to the estrogen receptors on Leydig cells they are able to be regulated by estrogen, but some authors debate whether changes in testosterone production are associated with down regulation of Leydig cell's testosterone production or a decrease in Leydig cell numbers after exposure to phytoestrogens^{77; 78}. I hypothesize it is some combination of both, and possibly associated with the topoisomerase inhibitor function of some isoflavones causing cell death, while the estrogenic capabilities of these isoflavones are impacting testosterone production.

4.4 Uterus

After interesting results in the placental FACS and Testes tissues, I opted to evaluate the uterus for inter-chromosomal HR. Female mice were treated with genistein at 250mg/kg/day for 28 days, and their uterus was extracted for analysis. Upon analysis it was observed that the genistein treated mice had small, isolated inter-chromosomal HR events between follicular columns, and occasionally in the epithelial cells lining the follicular spaces of the uterus. Although the untreated and genistein supplemented groups presented with more nuclei, this is likely due to size differences in the mice or regional differences in the tissue rather than the experimental conditions. The genistein supplemented mouse did present clotting in the fallopian tubes or potentially an infection of some kind; the exact cause of these morphological differences has not been determined, although it is clear there are excess red blood cells present. The Rainbow mice expressing I-SceI produced small regions of GFP clusters, which is potentially a clonally expanded group of proliferating cell types. It is known that the female reproductive tract is important to proper development of fetuses, and that phytoestrogens can act as endocrine disruptors. Genistein, which can mimic endogenous estradiol, has the potential to disrupt fertility because of this function⁸⁰. In an interesting observation, one of our two mice treated through gestation presented with uterine abnormalities, including clotting, thickened fallopian tubes, and other splotchiness in its appearance. Although the exact cause is undetermined, the pregnancy also appeared stunted in some way, with only one pup located halfway between the uterus and ovaries. It has been cited that adult female rodents have experienced poor development of the oviduct and a poor uterine environment for a developing fetus, and I hypothesize this has influenced the pregnancies of our mice as well, and may have contributed to why it has been so difficult to get in-utero mice to analyze for genistein exposure. There were several mice that presented with plugs initially, that did not proceed with pregnancy when treated with genistein before conception. Hence, the protocol was adjusted to begin genistein treatment post-conception, and less difficulty producing pregnant mice was observed. Further, it has been shown that

endocrine disruptors can increase the incidence of uterine fibroids during development. This is associated with changes in DNA repair in myometrial stem cells. The rats treated with endocrine disruptors experienced a decrease in the function of NHEJ, increased levels of DNA DSBs, and overall increased dysfunctionality in the DSB repair abilities of the myometrial stem cells. This malfunction in DNA DSB repair supports the idea that exposure to genistein has the ability to cause cellular stress, and increases in DSBs that may be resolved resulting in inter-chromosomal HR as observed in our data.

4.5 Significance and Implications

I have provided the first direct demonstration that genistein diet supplementation can promote *in vivo* inter-chromosomal HR events. These data have significant implications for diet-induced DNA damage, genome integrity, and chromosomal translocations associated with leukemias including infant leukemias. However not all tissues produced a robust number of GFP⁺ cells indicative of inter-chromosomal HR. It is not determined if this is a biologic reason due to inhibition of DSB induced HR repair, or if the dose was not acute enough, or the exposure time needs to be chronic to induce inter-chromosomal HR. Because of the rarity of genome instability, to see such destabilizing events it is also possible that a p53 deficiency or other immunoregulatory issues are required. It is also possible that the events created are below our level of detection using flowcytometry, and in this case we can also consider further immunohistochemistry. To reach a level of detectable events, it could be required to have increased cellular proliferation induced by the formation of pre-oncogenic or oncogenic mutations. It is also possible these events are too rare to see without high throughput single cell sequencing or digital droplet PCR. Other work could include the evaluation of bioflavonoid induced HR recombinants using high throughput single cell sequencing or digital droplet PCR. Further, our Rainbow mice could be crossed with mice p53 mutants, or other DNA damage repair mutants, to evaluate how the suppression of DNA damage regulatory systems may exacerbate genome instability induced by bioflavonoids, and may be the

destabilizing events required to see inter-chromosomal HR recombinants in these tissues. There is potentially a threshold dose responsible for mutagenesis that differs in each tissue. Future directions could also include genome-wide mapping breaks via sequencing in wild type mice. Further backtracking could include a comet assay to assess the overall damaging potential of genistein in eukaryotic cells. Previous work with comet assays has utilized a methodology via CometChip capable of detecting double strand breaks induced by chemicals, and assessing repair capacity⁸¹. Other in vivo studies have evaluated intra-chromosomal (same chromosome) DSB repair that does not have any implications for genome integrity and chromosomal translocations. In that study of the RaDR-GFP mouse, it was shown that chemical exposure can induce intrachromosomal HR⁸². Significantly, my work and the Rainbow mouse model extends those initial studies by demonstrating that these chemical and dietary supplementation can cause inter-chromosomal HR. This implies a more mutagenic role of genistein has previously been described and serves as important evidence that genistein supplementation should be moderated.

REFERENCES

1. A S, LA L-B, K U-K, S L. 2004. Molecular mechanisms of mammalian dna repair and the dna damage checkpoints. *Annu Rev Biochem.* p. 39-85.
2. Chatterjee N, Walker GC. Mechanisms of dna damage, repair and mutagenesis.
3. Ciccia A, Elledge SJ. 2010. The dna damage response: Making it safe to play with knives. *NIH Public Access.* p. 179.
4. A C, C M. 2020. Dna damage: From threat to treatment. *Cells.*
5. Bartek J. 2011. Dna damage response, genetic instability and cancer: From mechanistic insights to personalized treatment. *Wiley-Blackwell.* p. 303.
6. Krokan HE, Bjoras M. 2013. Base excision repair. *Cold Spring Harbor Perspectives in Biology.* 5(4):a012583-a012583.
7. Scharer OD. 2013. Nucleotide excision repair in eukaryotes. *Cold Spring Harbor Perspectives in Biology.* 5(10):a012609-a012609.
8. Kunkel TA, Erie DA. 2005. Dna mismatch repair. *Annual Review of Biochemistry.* 74(1):681-710.
9. Jasin M, Rothstein R. 2013. Repair of strand breaks by homologous recombination. *Cold Spring Harbor Laboratory Press.*
10. Kass EM, , Helgadottir HR, , Chen CC, , Barbera M, , Wang R, et al. 2013. Double-strand break repair by homologous recombination in primary mouse somatic cells requires brca1 but not the atm kinase. p. 5564-5569.
11. Burma S, Chen BPC, Chen DJ. 2006. Role of non-homologous end joining (nhej) in maintaining genomic integrity. p. 1042-1048.
12. A U, N C, A Y. 2020. Relationship among dna double-strand break (dsb), dsb repair, and transcription prevents genome instability and cancer. *Cancer Sci.* p. 1443-1451.
13. AbdulSalam SF, Thowfeik FS, Merino EJ. 2016. Excessive reactive oxygen species and exotic dna lesions as an exploitable liability. *Biochemistry.* p. 5341-5352.
14. Ceccaldi R, Rondinelli B, D'Andrea AD. 2016. Repair pathway choices and consequences at the double-strand break. *Elsevier Ltd.* p. 52-64.
15. Chang HHY, Pannunzio NR, Adachi N, Lieber MR. 2017. Non-homologous dna end joining and alternative pathways to double-strand break repair. *NIH Public Access.* p. 495.
16. Guirouilh-Barbat J, Lambert S, Bertrand P, Lopez BS, Porro A, Chang M, Research E. 2014. Is homologous recombination really an error-free process?
17. San Filippo J, Sung P, Klein H. 2008. Mechanism of eukaryotic homologous recombination. *Annu Rev Biochem.* p. 229-257.
18. Grelon M. 2016. Meiotic recombination mechanisms. No longer published by Elsevier. p. 247-251.
19. Mazin AV, Kowalczykowski SC. 1999. A novel property of the recA nucleoprotein filament: Activation of double- stranded dna for strand exchange in trans. *Genes & Development.* 13(15):2005-2016.
20. Lamarche BaJ, Orazio NI, Weitzman MD. The mrn complex in double-strand break repair and telomere maintenance.
21. Li W, Li F, Huang Q, Shen J, Wolf F, He Y, Liu X, Hu YA, Bedford JS, Li CY. 2011. Quantitative, noninvasive imaging of radiation-induced dna double-strand breaks *in vivo*. p. 4130-4137.
22. Li X, , Heyer W-D, . 2008. Homologous recombination in dna repair and dna damage tolerance. p. 99-113.
23. Wright WD, Shah SS, Heyer WD. 2018. Homologous recombination and the repair of dna double-strand breaks. *Elsevier.* p. 10524-10535.

24. McClendon AK, Osheroff N. 2007. Dna topoisomerase ii, genotoxicity, and cancer. NIH Public Access. p. 83.
25. Pommier Y, Leo E, Zhang H, Marchand C. 2010. Dna topoisomerases and their poisoning by anticancer and antibacterial drugs. p. 421-433.
26. Felix CA, Kolaris CP, Osheroff N. 2006. Topoisomerase ii and the etiology of chromosomal translocations. p. 1093-1108.
27. Cobb J, Reddy RK, Park C, Handel MA. 1997. Analysis of expression and function of topoisomerase i and ii during meiosis in male mice. *Molecular Reproduction and Development*. 46(4):489-498.
28. Azarova AM, Lyu YL, Lin CP, Tsai YC, Lau JYN, Wang JC, Liu LF. 2007. From the cover: Roles of dna topoisomerase ii isozymes in chemotherapy and secondary malignancies. *National Academy of Sciences*. p. 11014.
29. de Campos-Nebel M, Larripa I, González-Cid M. 2010. Topoisomerase ii-mediated dna damage is differently repaired during the cell cycle by non-homologous end joining and homologous recombination. p. 1-13.
30. Ling EM, Baslé A, Cowell IG, Van Den Berg B, Blower TR, Austin CA. 2022. A comprehensive structural analysis of the atpase domain of human dna topoisomerase ii beta bound to amppnp, adp, and the bisdioxopiperazine, icrf193. p. 1129-1145.e1123.
31. Burden DA, Osheroff N. 1998. Mechanism of action of eukaryotic topoisomerase ii and drugs targeted to the enzyme. *Elsevier*. p. 139-154.
32. Gruhn JR, Al-Asmar N, Fasnacht R, Maylor-Hagen H, Peinado V, Rubio C, Broman KW, Hunt PA, Hassold T. 2016. Correlations between synaptic initiation and meiotic recombination: A study of humans and mice. *Am J Hum Genet*. p. 102-115.
33. Hassold T, Sherman S, Hunt P. 2000. Counting cross-overs: Characterizing meiotic recombination in mammals. *Hum Mol Genet*. p. 2409-2419.
34. Hunter N. 2015. Meiotic recombination: The essence of heredity. *Cold Spring Harb Perspect Biol*.
35. Cowell IG, Sondka Z, Smith K, Lee KC, Manville CM, Sidoreczuk-Lesthuruge M, Rance HA, Padget K, Jackson GH, Adachi N et al. 2012. Model for mll translocations in therapy-related leukemia involving topoisomerase ii β -mediated dna strand breaks and gene proximity. p. 8989-8994.
36. Bande OJ, Osheroff N. 2008. The efficacy of topoisomerase ii-targeted anticancer agents reflects the persistence of drug-induced cleavage complexes in cells. p. 11900-11908.
37. Skok Ž, Zidar N, Kikelj D, Ilaš J. 2020. Dual inhibitors of human dna topoisomerase ii and other cancer-related targets. *American Chemical Society*. p. 884-904.
38. Britten O, Ragusa D, Kosi S, Kamel YM. 2019. Mll-rearranged acute leukemia with t(4;11)(q21;q23)—current treatment options. Is there a role for car-t cell therapy? : *Multidisciplinary Digital Publishing Institute*. p. 1341.
39. Bariar B, , Vestal CG, , Deem B, , Goodenow D, , Ughetta M, et al. 2019. Bioflavonoids promote stable translocations between mll-af9 breakpoint cluster regions independent of normal chromosomal context: Model system to screen environmental risks. *John Wiley and Sons Inc*. p. 154-167.
40. Panche AN, Diwan AD, Chandra SR. 2016. Flavonoids: An overview. p. 1-15.
41. Ross JA. Dietary flavonoids and the mll gene: A pathway to infant leukemia?
42. Ross JA, Kasum CM. 2002. Dietary flavonoids: Bioavailability, metabolic effects, and safety. p. 19-34.
43. Yu T, Huang D, Wu H, Chen H, Chen S, Cui Q. 2021. Navigating calcium and reactive oxygen species by natural flavones for the treatment of heart failure.: *Frontiers Media S.A.* p. 718496.
44. Messina M, Duncan A, Messina V, Lynch H, Kiel J, Erdman JW. 2022. The health effects of soy: A reference guide for health professionals.: *Frontiers Media S.A.* p. 970364.

45. Williamson G. 2017. The role of polyphenols in modern nutrition. Wiley-Blackwell. p. 226.
46. Williamson-Hughes PS, Flickinger BD, Messina MJ, Empie MW. 2006. Isoflavone supplements containing predominantly genistein reduce hot flash symptoms: A critical review of published studies. *Menopause*. p. 831-839.
47. Nowak D, Gośliński M. 2020. Assessment of antioxidant properties of classic energy drinks in comparison with fruit energy drinks. Multidisciplinary Digital Publishing Institute (MDPI).
48. Campbell B, Wilborn C, La Bounty P, Taylor L, Nelson MT, Greenwood M, Ziegenfuss TN, Lopez HL, Hoffman JR, Stout JR et al. 2013. International society of sports nutrition position stand: Energy drinks. Taylor & Francis. p. 1.
49. Yu L, Rios E, Castro L, Liu J, Yan Y, Dixon D. 2021. Genistein: Dual role in women's health. Multidisciplinary Digital Publishing Institute (MDPI).
50. Zin SRM, Omar IZ, Khan ILA, Musameh II, Das I, Kassim IM. 2013. Effects of the phytoestrogen genistein on the development of the reproductive system of sprague dawley rats. *Clinics*. 68:253-262.
51. Stijns M, Ogata F, Godschalk RWL, Vanhees K, Limburg UB, Ziekenhuis J, Sahar B, Van Waalwijk Van Doorn-Khosrovani B. 2022. Maternal exposure to genistein during pregnancy and oxidative dna damage in testes of male mouse offspring.: *Frontiers Media SA*. p. 904368-904368.
52. Barjesteh Van Waalwijk Van Doorn-Khosrovani S, Janssen J, Maas LM, Godschalk RWL, Nijhuis JG, Van Schooten FJ. 2007. Dietary flavonoids induce mll translocations in primary human cd34 1 cells. p. 1703-1709.
53. Goodenow D, Emmanuel F, Berman C, Sahyouni M, Richardson C. 2020. Bioflavonoids cause dna double-strand breaks and chromosomal translocations through topoisomerase ii-dependent and -independent mechanisms. Elsevier B.V.
54. Azarova, Lin RK, Tsai YC, Liu LF, Lin CP, Lyu YL. 2010. Genistein induces topoisomerase ii beta- and proteasome-mediated dna sequence rearrangements: Implications in infant leukemia. NIH Public Access. p. 66.
55. Doerge DR, Churchwell MI, Chang HC, Newbold RR, Delclos KB. 2001. Placental transfer of the soy isoflavone genistein following dietary and gavage administration to sprague dawley rats. *Reprod Toxicol*. p. 105-110.
56. Wang S, Maxwell CA, Akella NM. 2021. Diet as a potential moderator for genome stability and immune response in pediatric leukemia. *Cancers (Basel)*. p. 1-17.
57. Furness DLF, Dekker GA, Roberts CT. 2011. Dna damage and health in pregnancy. *J Reprod Immunol*. p. 153-162.
58. Bhagwat S, Haytowitz DB, Holden JM. 2008. Usda database for the isoflavone content of selected foods, release 2.0. Maryland: US Department of Agriculture. 15.
59. Strom BL, Schinnar R, Ziegler EE, Barnhart KT, Sammel MD, Macones GA, Stallings VA, Drulis JM, Nelson SE, Hanson SA. 2001. Exposure to soy-based formula in infancy and endocrinological and reproductive outcomes in young adulthood. *Jama*. 286(7):807-814.
60. Vanhees K, Van Schooten FJ, Van Waalwijk Van Doorn-Khosrovani SB, Van Helden S, Munia A, Peluso M, Briedé JJ, Haenen GRMM, Godschalk RWL. 2013. Intrauterine exposure to flavonoids modifies antioxidant status at adulthood and decreases oxidative stress-induced dna damage. *Free Radic Biol Med*. p. 154-161.
61. Morris SM, Akerman GS, Warbritton A, Patton RE, Doerge DR, Ding X, Chen JJ. 2003. Effect of dietary genistein on cell replication indices in c57bl6 mice. Elsevier Ireland Ltd. p. 139-145.
62. Jefferson WN, Padilla-Banks E, Newbold RR. 2005. Adverse effects on female development and reproduction in cd-1 mice following neonatal exposure to the phytoestrogen genistein at environmentally relevant doses. *Biol Reprod*. p. 798-806.

63. Wu G, Wei Q, Yu D, Shi F. 2019. Neonatal genistein exposure disrupts ovarian and uterine development in the mouse by inhibiting cellular proliferation. *J Reprod Dev.* p. 7-17.
64. Olubajo Awobajo F, , Aderonke Samuel T, , Olufemi Morakinyo A, , Tinuolaoluwa Oyelowo O, , Uzoamaka Onyekwele P, et al. Aberrant effect of genistein on placenta development expressed through alteration in transforming growth factor- β 1 and alkaline phosphatase across the maternal serum, the placenta and the amniotic fluid.
65. Huang Q, Braffett BH, Simmens SJ, Young HA, Ogden CL. 2020. Dietary polyphenol intake in us adults and 10-year trends: 2007-2016. *J Acad Nutr Diet.* p. 1821-1833.
66. Yellayi S, Naaz A, Szewczykowski MA, Sato T, Woods JA, Chang J, Segre M, Allred CD, Helferich WG, Cooke PS. 2002. The phytoestrogen genistein induces thymic and immune changes: A human health concern? *Proceedings of the National Academy of Sciences.* 99(11):7616-7621.
67. Setchell KD. 2006. Assessing risks and benefits of genistein and soy. *Environ Health Perspect.* 114(6):A332-333.
68. Rogers AB, Dintzis RZ. 2018. 13 - hepatobiliary system. In: Treuting PM, Dintzis SM, Montine KS, editors. *Comparative anatomy and histology* (second edition). San Diego: Academic Press. p. 229-239.
69. Sudan S, Rupasinghe HPV. 2014. Flavonoid-enriched apple fraction af4 induces cell cycle arrest, dna topoisomerase ii inhibition, and apoptosis in human liver cancer hepg2 cells. *Nutrition and Cancer.* 66(7):1237-1246.
70. Hayashi K, Hishikawa A, Itoh H. 2019. Dna damage repair and dna methylation in the kidney. *American Journal of Nephrology.* 50(2):81-91.
71. Gupta N, Matsumoto T, Hiratsuka K, Garcia Saiz E, Zhang C, Galichon P, Miyoshi T, Susa K, Tatsumoto N, Yamashita M et al. 2022. Modeling injury and repair in kidney organoids reveals that homologous recombination governs tubular intrinsic repair. *Science Translational Medicine.* 14(634):eabj4772.
72. Heim M, Frank O, Kampmann G, Sochocky N, Pennimpede T, Fuchs P, Hunziker W, Weber P, Martin I, Bendik I. 2004. The phytoestrogen genistein enhances osteogenesis and represses adipogenic differentiation of human primary bone marrow stromal cells. *Endocrinology.* 145(2):848-859.
73. Ishimi Y, Yoshida M, Wakimoto S, Wu J, Chiba H, Wang X, Takeda K, Miyaura C. 2002. Genistein, a soybean isoflavone, affects bone marrow lymphopoiesis and prevents bone loss in castrated male mice. *Bone.* 31(1):180-185.
74. Li M, Yu Y, Xue K, Li J, Son G, Wang J, Qian W, Wang S, Zheng J, Yang C et al. 2023. Genistein mitigates senescence of bone marrow mesenchymal stem cells via $\text{err}\alpha$ -mediated mitochondrial biogenesis and mitophagy in ovariectomized rats. *Redox Biol.* 61:102649.
75. Coorens THH, Oliver TRW, Sanghvi R, Sovio U, Cook E, Vento-Tormo R, Haniffa M, Young MD, Rahbari R, Sebire N et al. 2021. Inherent mosaicism and extensive mutation of human placentas. *Nature.* 592(7852):80-85.
76. Awobajo FO, Samuel TA, Morakinyo AO, Oyelowo OT, Onyekwele PU, Medobi EF, Abdul MW, Aminu BB, Oruade EO. 2020. Aberrant effect of genistein on placenta development expressed through alteration in transforming growth factor- β 1 and alkaline phosphatase across the maternal serum, the placenta and the amniotic fluid. *Iran J Basic Med Sci.* 23(10):1301-1306.
77. Akingbemi BT, Braden TD, Kempainen BW, Hancock KD, Sherrill JD, Cook SJ, He X, Supko JG. 2007. Exposure to phytoestrogens in the perinatal period affects androgen secretion by testicular leydig cells in the adult rat. *Endocrinology.* 148(9):4475-4488.
78. Opalka DM, Kaminska B, Piskula MK, Puchajda-Skowronska H, Dusza L. 2006. Effects of phytoestrogens on testosterone secretion by leydig cells from biłgoraj ganders (anser anser). *Br Poult Sci.* 47(2):237-245.

79. Zhu Y, Xu H, Li M, Gao Z, Huang J, Liu L, Huang X, Li Y. 2016. Daidzein impairs leydig cell testosterone production and sertoli cell function in neonatal mouse testes: An in vitro study. *Molecular Medicine Reports*. 14(6):5325-5333.
80. Whirledge SD, , Kisanga EP, , Oakley RH, , Cidlowski JA, . 2018. Neonatal genistein exposure and glucocorticoid signaling in the adult mouse uterus. *Environ Health Perspect*. p. 047002-047001-047002-047017.
81. Weingeist DM, Ge J, Wood DK, Mutamba JT, Huang Q, Rowland EA, Yaffe MB, Floyd S, Engelward BP. 2013. Single-cell microarray enables high-throughput evaluation of dna double-strand breaks and dna repair inhibitors. *Cell Cycle*. 12(6):907-915.
82. Sukup-Jackson MR, Kiraly O, Kay JE, Na L, Rowland EA, Winther KE, Chow DN, Kimoto T, Matsuguchi T, Jonnalagadda VS et al. 2014. Rosa26-gfp direct repeat (radr-gfp) mice reveal tissue- and age-dependence of homologous recombination in mammals *in vivo*. *Public Library of Science*.
83. Caddle LB, Hasham MG, Schott WH, Shirley BJ, Mills KD. 2008. Homologous recombination is necessary for normal lymphocyte development. *Mol Cell Biol*. 28(7):2295-2303.
84. Richardson C, Jasin M. 2000. Frequent chromosomal translocations induced by dna double-strand breaks. *Nature*. 405(6787):697-700.